The Palaeobotanist 68(2019): 173–205
0031–0174/2019

Ordovician land plants and fungi from Douglas Dam, Tennessee

GREGORY J. RETALLACK

Department of Earth Sciences, University of Oregon, Eugene, OR 97403, USA.
**Email: gregr@uoregon.edu*

(Received 09 September, 2019; revised version accepted 15 December, 2019)

ABSTRACT

Retallack GJ 2019. Ordovician land plants and fungi from Douglas Dam, Tennessee. The Palaeobotanist 68(1–2): 173–205.

Ordovician land plants have long been suspected from indirect evidence of fossil spores, plant fragments, carbon isotopic studies, and paleosols, but now can be visualized from plant compressions in a Middle Ordovician (Darriwilian or 460 Ma) sinkhole at Douglas Dam, Tennessee, U. S. A. Five bryophyte clades and two fungal clades are represented: hornwort (*Casterlorum crispum*, new form genus and species), liverwort (*Cestites mirabilis* Caster & Brooks), balloonwort (*Janegraya sibylla*, new form genus and species), peat moss (*Dollyphyton boucotii*, new form genus and species), harsh moss (*Edwardsiphyton ovatum*, new form genus and species), endomycorrhiza (*Palaeoglomus strotheri*, new species) and lichen (*Prototaxites honeggeri*, new species). The Douglas Dam Lagerstätte is a benchmark assemblage of early plants and fungi on land. Ordovician plant diversity now supports the idea that life on land had increased terrestrial weathering to induce the Great Ordovician Biodiversification Event in the sea and latest Ordovician (Hirnantian) glaciation.

Key–words—Bryophyta, Fungi, Mycorrhizae, Darriwilian, Lenoir Limestone.

डॉगलस बांध (डैम), टेन्नेस्सी से प्राप्त ऑर्डोविशन भू–वनस्पतियां एवं कवक

ग्रेगॉरी जे. रेटलेक

सारांश

ऑर्डोविशन भू–वनस्पतियां जीवाश्म जीवाणुओं, वनस्पति खंडजों कार्बन समस्थानिक अध्ययनों व पुरानिखातों के परोक्ष प्रमाण से प्राप्त समझी गई हैं परंतु अब डॉगलस बांध, टेन्नेस्सी, यू.एस.ए. पर मध्य ऑर्डोविशन (डार्रीविलियन या 4 करोड़ 60 लाख) विलयन रंध्र में वनस्पति संपीडाश्मों से कल्पित की जा सकती हैं। पांच ब्रायोफाइट क्लेड एवं दो कवकी क्लेडः हॉर्नवर्ट (*केस्टरलोरम क्रिस्पम,* वंश व जाति नूतन रूप), लिवरवर्ट (*सेस्टिटीज मिराबिलिस* केस्टर एवं ब्रुक्स), बैलूनवर्ट (*जनेग्रेया सिबील्ला,* वंश व जाति नूतन रूप), पीट मॉस (*डॉलीफायटन बौकोटयाई,* वंश व जाति नूतन रूप) कर्कश मॉस (*एडवर्डसिफीटन ओवेटम,* वंश व जाति नूतन रूप), एंडोमाइकॉर्रहिज़ा (*पैलियोग्लोमस स्ट्रोतेरी,* नूतन जाति) और लाइकैन (*प्रोटोटैक्साइटीज होनेग्गेरी,* नूतन जाति) रूपायित हुई हैं। डॉगलस बांध (डैम) लैजरस्टेटी स्थल पर प्रारंभिक वनस्पतियों व कवक का तलचिह्न समुच्चय है। ऑर्डोविशन वनस्पति विविधता अब इस विचार का समर्थन करती है कि सागर एवं अद्यतन ऑर्डोविशन (हिर्नेनटियन) हिमनदन में बृहत ऑर्डोविशन जैवविविधरूपण घटना अनुमानित करने को स्थल पर जीवन स्थलीय अपक्षय बढ़ा।

सूचक शब्द—ब्रायोफाइटा, कवक, मायकॉर्रहिज़े, डार्रीविलियन लेनॉइर चूनापत्थर।

INTRODUCTION

LATE Silurian is still regarded as a benchmark for the first appearance of land plants and consequent landscape modernization (McMahon & Davies, 2018), despite mounting circumstantial evidence to the contrary (Wellman *et al*., 2003; Tomescu *et al*., 2009; Retallack, 2015a; Steemans & Wellman, 2018; Morris *et al.*, 2018). Because previously described Ordovician plant megafossils have been regarded as uninformative (Pant & Bhowmik, 1998; Taylor *et al.*, 2009), the evolutionary origin of land plants remains obscure (Morris *et al.*, 2018), embryophyte molecular clocks are insecure (Puttick *et al.*, 2018), and the role of plants in global change is unclear (Porada *et al.*, 2016). What is needed is an Ordovician

terrestrial Lagerstätte, like the Early Devonian Rhynie Chert (Taylor *et al.*, 2009; Krings *et al.*, 2017) or Barzass Coal (Krassilov, 1981). Such a deposit has been hiding in plain sight for the past 62 years in a monograph on the articulated fossil arthropods *Chasmataspis laurenci* and *Douglasiocaris collinsi* of the Douglas Dam Lagerstätte (Caster & Brooks, 1956), which is the site for all material described here.

Ordovician land plants have been controversial (Taylor *et al.*, 2009), despite a local abundance of material (Lesquereux, 1874, 1877; Fritsch, 1908; Kozlowski & Greguss, 1959;

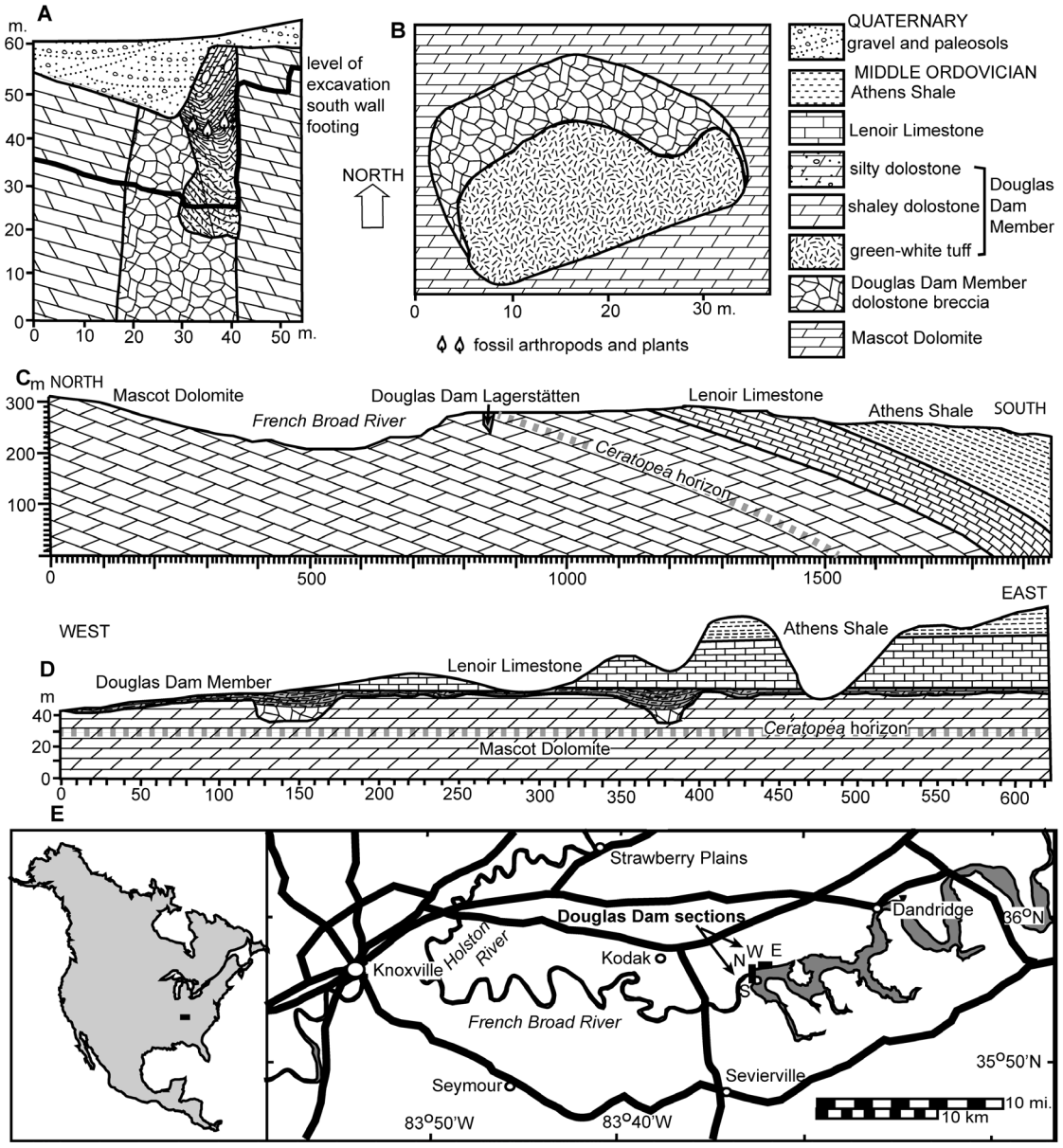

Fig. 1—Location of Douglas Dam and dolostones of Early Ordovician Knox Group, with paleokarst visible in geological cross sections (Laurence 1944, Bridge 1955): (A) vertical cross section of the fossiliferous sinkhole showing level of fossils; (B) horizontal plan of the sinkhole at the level of the green tuff; (C) north–south geological section showing the fossiliferous sinkhole; (D) east–west geological section showing other sinkholes of the paleokarst on Mascot Dolomite; (E) location of fossiliferous sinkhole and geological cross sections.

Fig. 2—Douglas Dam locality, matrix and tracks; (A), Douglas Lake (left) and French Broad River (right), Sevier County, Tennessee in 2016, showing south end of dam covering the fossiliferous cenote–fill of Douglas Dam Member of the Lenoir Limestone, Middle Ordovician (Darriwilian, 460 Ma); (B–C), ripple marks in core of Douglas Dam Member; (D), desiccation cracks and rooting structures in vertical thin section; (E), oversize dolostone clast in varved shale of vertical thin section; (F), rooting structures in horizontal thin section, (G–H), arthropod tracks of *Diplichnites gouldi* (Gevers) Bradshaw 1981. Cores in Smithsonian are from levels 913.0–913.1 ft (B) and 912.8–912 ft (C) levels. Specimens are PB2255 (D,F), PB 2279 (E), and USNM645800A–B (G–H). Scale bars are in mm.

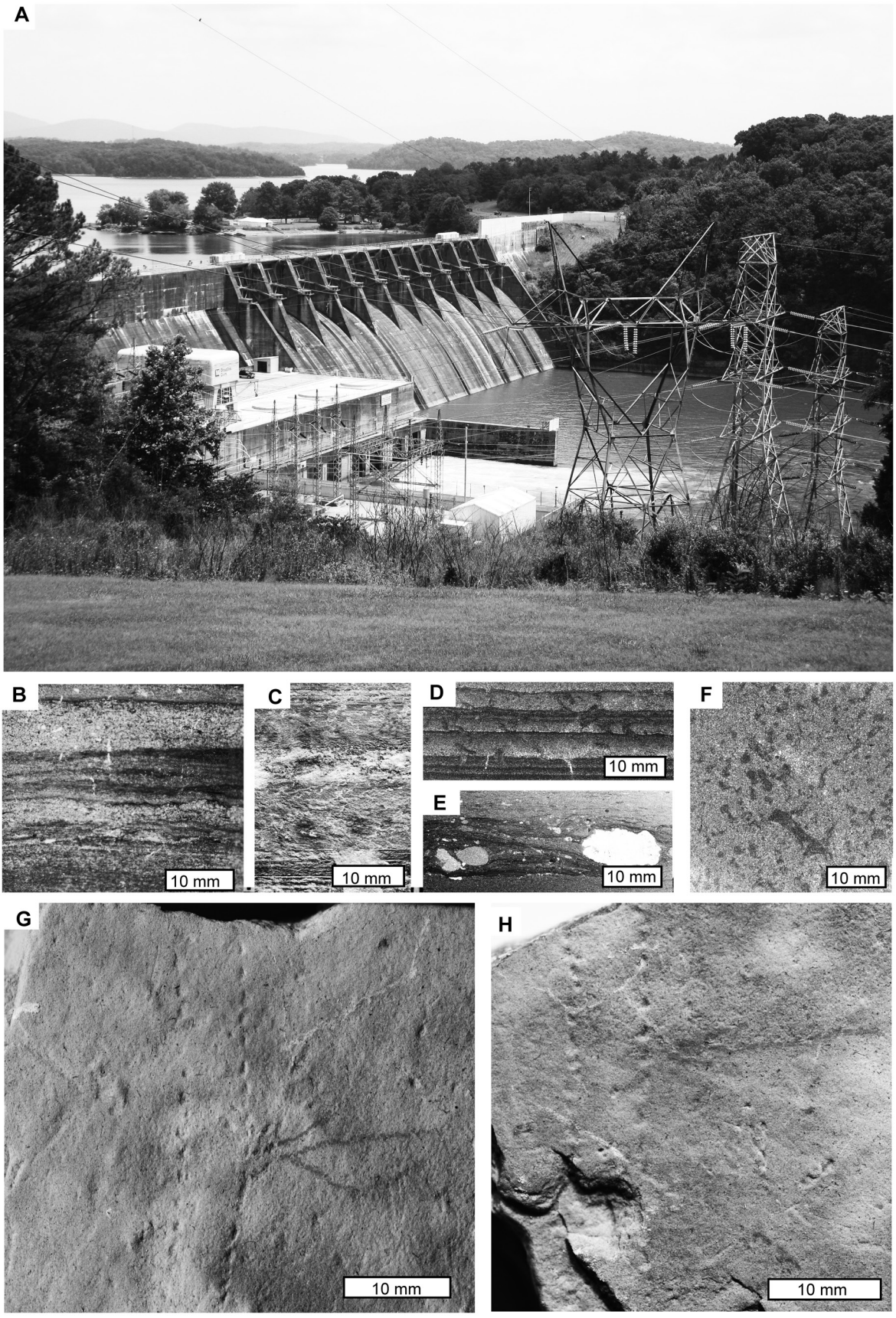
A
B
10 mm
C
10 mm
D
10 mm
E
10 mm
F
10 mm
G
10 mm
H
10 mm

Greguss, 1962; Arbey & Koeniguer, 1979; Snigirevskaya *et al*., 1992; Salamon *et al*., 2018). One problem highlighted by debate between Banks (1975) and Gray & Boucot (1972, 1977) is that Ordovician vegetation was mainly unfamiliar non–vascular plants. The oldest known vascular land plant megafossils are still no older than Middle Silurian *Baragwanathia longifolia* found with *Bohemograptus bohemicus* graptolites (426 Ma) from Yea, Australia (Rickards, 2000), and *Cooksonia barrandei* in the *Monograptus belophorus* graptolite zone (432 Ma) from Loděnice, Czech Republic (Libertin *et al*., 2018). The idea that land was barren of plants before Silurian has been promoted by reviews emphasizing quality of preservation in fossil plants of Silurian or younger age (Taylor *et al*., 2009; Krings *et al*., 2017), and outlining changing architecture of selected alluvial deposits by Silurian–Devonian (Davies *et al*., 2011; McMahon & Davies, 2018).

A contrary narrative has emerged as studies of Ordovician spores established their bryophytic, and thus non–vascular plant affinities (Vavrdová, 1984; Gray, 1985; Nøhr–Hansen & Koppelhus, 1988; Taylor, 1996, 1997; Wellman & Gray, 2000; Steemans *et al.*, 2009, 2010), and extended their range back to Early Ordovician (Gray *et al*., 1982; Rubenstein *et al.*, 2010; Kenrick *et al.*, 2012; Vecoli *et al.*, 2017), and perhaps Middle Cambrian (Taylor & Strother, 2008, 2009; Strother, 2016). Ordovician spores also have been found within sporangial remnants lacking vegetative details (Wellman *et al*., 2003). Molecular data on modern plants now indicates a Cambrian to Early Ordovician origin of non–vascular land plants (Morris *et al.*, 2018). Ordovician and Cambrian land plant spores remain problematic and may represent pre–bryophytic lineages, but the alternative terms cryptospores and cryptophytes (Edwards *et al*., 2014), enshrine rather than dispel the mystery. There is also evidence from palynology for Middle Ordovician glomalean fungi (Redecker *et al.,* 2000, 2002), and other Glomeromycota may be represented by Ediacaran acritarchs (Retallack, 2015b), and Proterozoic megafossils (Retallack *et al.*, 2013a, 2013b, 2018). Evidence of Cambrian and Ordovician land plants also comes from carbon isotopic composition of carbonaceous debris and sediments (Tomescu & Rothwell, 2006; Tomescu *et al.*, 2009), and from chemical and textural profile differentiation of clayey Cambrian and Ordovician paleosols (Retallack, 2008, 2009, 2015a). Despite this circumstantial evidence for Ordovician vegetation, the macroscopic appearance, diversity and taxonomic affinities of Ordovician megafossils remained elusive until now.

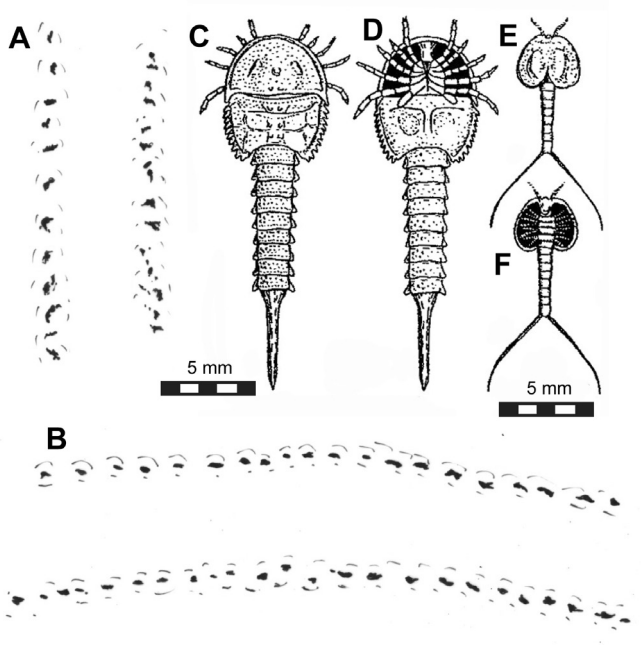

Fig. 3—Reconstructions of Middle Ordovician (Darriwilian) arthropods from the Douglas Dam Member of the Lenoir Limestone in a palaeocenote excavated during construction of Douglas Dam, Tennessee: (A–B), trackway *Diplichnites gouldi* (Gevers) Bradshaw 1981; (C–D),*Chasmataspis laurenci* Caster & Brooks 1956; (E–F), *Douglasiocaris collinsi* Caster & Brooks 1956.

GEOLOGICAL SETTING

The source of the plant and arthropod fossils is a small (9 m wide, by 27 m long, and 90 m deep) fissure fill within Mascot Dolomite of the Knox Group, now completely covered by the southern footing of Douglas Dam, Sevier County, Tennessee (Figs 1–2A). The fossiliferous beds then were 20 m below the surface and were entirely removed down to the underlying volcanic ash, covered during construction of the dam for the Tennessee Valley Authority in 1942, and mapped in detail during construction (Laurence, 1944; Bridge, 1955). The north side of the sinkhole has syndepositional dolostone breccia, which may have formed a talus cone and filled the base of the paleodoline. The south side of the sinkhole was filled at first with 12 m of white volcanic ash, and then 8 m of green volcanic ash. The fossiliferous level of 6 m of varved shale and silty dolostone was thus 70–64 m below the dolostone paleoplateau. The best preservation of plants and arthropods is in carbonaceous shaley laminae at this stratigraphic level. This fossiliferous layer is covered by 12 m of flaggy limestones, with some 52 m of additional Douglas Dam Member of the Lenoir Limestone eroded above that, and covered by Quaternary terrace gravels before dam excavation. Macerated fossil fragments and spores are dark brown, compatible with conodont alteration index of 3–4 for enclosing rocks due to 2.7–5.5 km of rock overburden and burial temperatures of 100–200ºC **(**Epstein *et al*., 1977**)**. Thermal maturity and unweathered matrix from excavation to a depth of 20 m rules out contamination by surface spores.

Elsewhere in this area, paleorelief on the Mascot Dolomite is no more than 42 m, and filled with red beds or light gray limestones (Bridge, 1955; Walker *et al.*, 1992). These shallower parts of the paleorelief were filled with

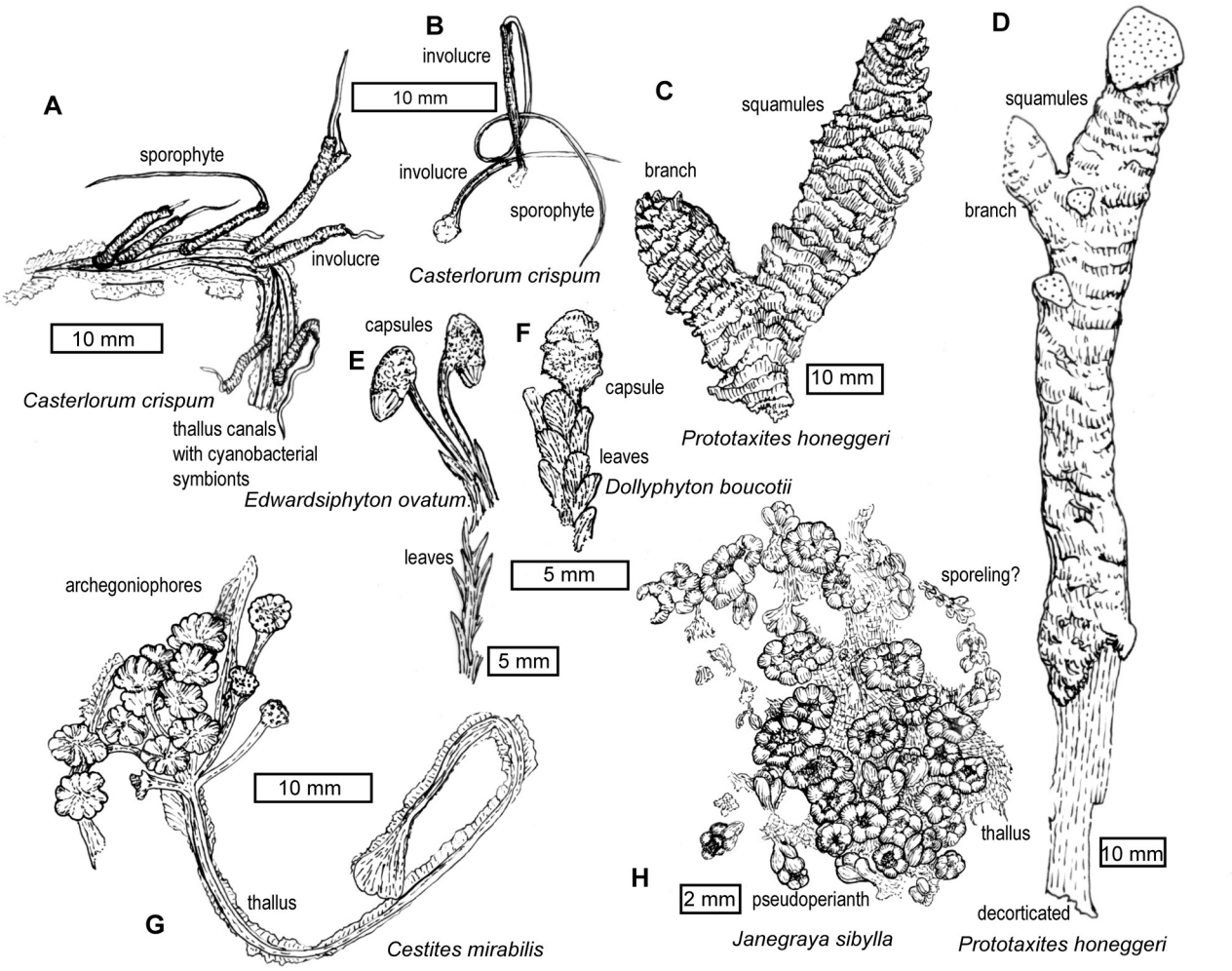

Fig. 4—Interpretive and annotated sketches of the Middle Ordovician (Darriwilian) non–vascular land plant specimens from the Douglas Dam Member of the Lenoir Formation under Douglas Dam, Tennessee: (A–B), *Casterlorum crispum* new genus and species (A=holotype), hornwort: (C–D), *Prototaxites honeggeri* new species (C=holotype), extinct nematophyte: (E), *Edwardsiphyton ovatum* new genus and species (holotype), peat moss; (F), *Dollyphyton boucotii* new genus and species (holotype), harsh moss; (G), *Cestites mirabilis* Caster & Brooks 1956, liverwort: (H), *Janegraya sibylla* new genus and species (holotype), balloonwort. Specimens are USNM125102 (A), USNMI128089 (B), USNM125084 (C), USNM125083 (D), PB2281 (E), PB2275 (F), PB2266 (G), PB2254 (H).

limestones of the upper Douglas Dam Member containing an estuarine fauna of rhynchonellid (*Rostricella pristina*) and lingulid brachiopods (*Lingula fostermontanensis*). Above that level, in the uppermost Douglas Dam Member of the Lenoir Limestone are normal marine faunas of Darriwilian age (460 Ma), including the brachiopods *Rafinesquina champlainensis, Valcourea strophomenoides*, *Hesperorthis* sp. and *Mimella* sp. Sandy to clayey limestones of the overlying Mosheim Member of the Lenoir Limestone have marine gastropods *Lophospira* sp. and *Maclurites magna* (Neuman, 1955). These represent a substantial marine transgression in the region (Herrmann & Haynes, 2015). Geological age of the fossil plants is thus bracketed by Mascot Dolomite of the Knox Group (Floian, 470 Ma), and the disconformably overlying Lenoir Limestone (Darriwilian, 459 Ma). The age of the plant fossils is thus about 460 Ma, because deposition of the non–marine Douglas Dam Member is continuous upwards into the marine Mosheim Member (Bridge, 1955).

Additional indications of age may come from tuffs below the fossiliferous level within the sinkhole, which are lithic tuffs unusual for Ordovician k–bentonites (Laurence, 1944). They are lithologically distinct from Dieke and Millbrig k–bentonites of Middle Ordovician age (453 Ma: Huff & Turkmenoglu, 1981; Huff, 1983, 2008; Huff *et al*., 1992; Min *et al*., 2001; Sell *et al.*, 2015). A likely correlation (by Laurence, 1944) is with tuffs near the base of the Murfreesboro Limestone of Tennessee (Fox & Grant, 1944), now dated at about 464 Ma (Huff *et al*., 2010). Also possible

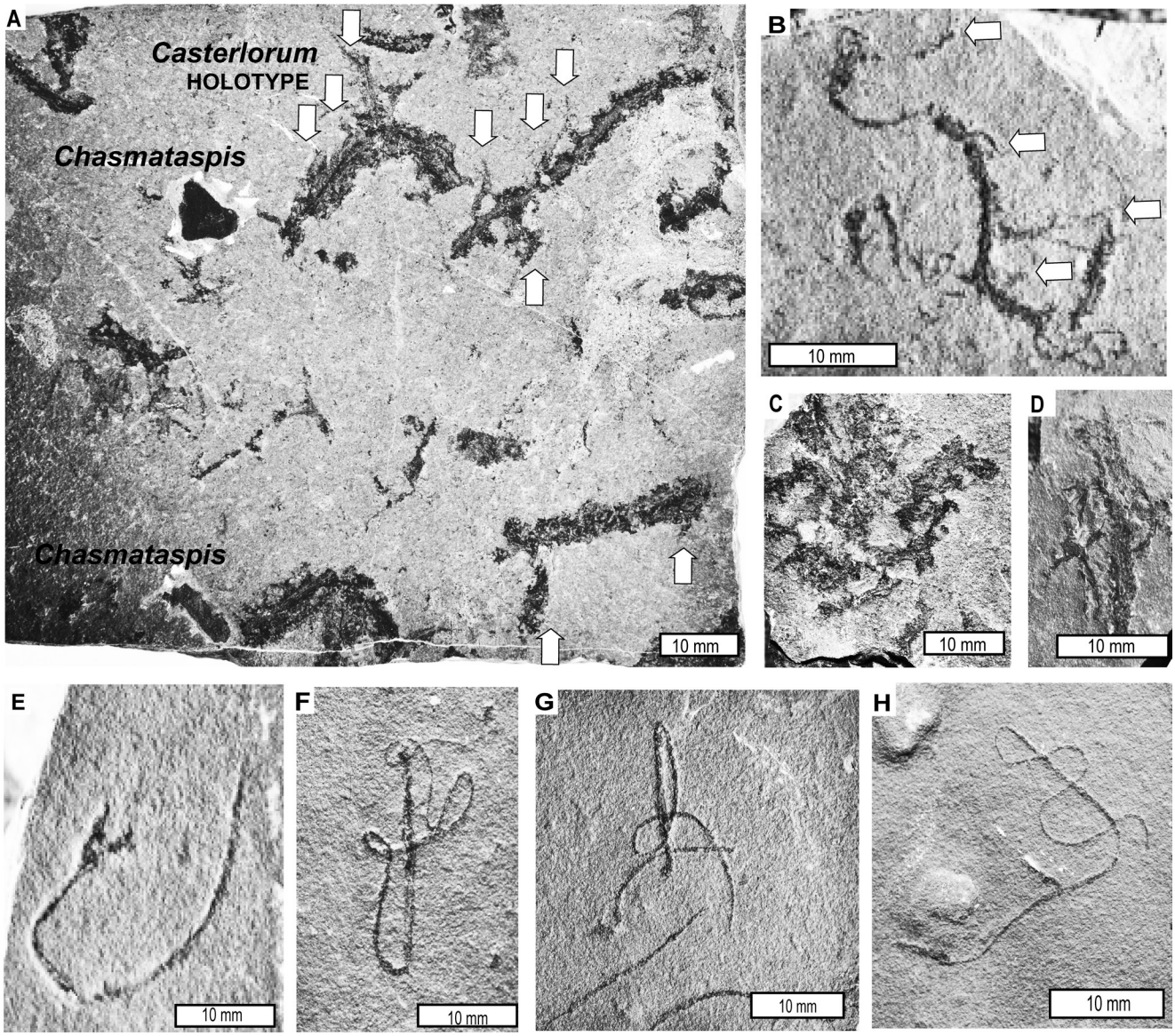

Fig. 5—*Casterlorum crispum* new genus and species from the Middle Ordovician (Darriwilian) Douglas Dam Member, Tennessee, with horns (obvious ones at arrows), and associated glossy carapace fragments of *Chasmataspis laurenci*; (A–D), thalloid gametophytes with dark apically dichotomizing lines and attached horns: (E–H), whip like dehisced sporangia, many with remnants of dark involucre at base; Specimens are USNM125102 (A), PB2254 (B), USNM125165 (C), USNM645552 (D), PB2252 (E), USNM128088 (F), USNM128089 (G); USNM128090 (H).

Fig. 6—*Casterlorum crispum* new genus and species from the Middle Ordovician (Darriwilian) Douglas Dam Member, Tennessee; (A–C), details of horns and basal involucres; (D), thallus with involucre bases and some fine rhizoids; (E–G), dark,apically dichotomozing lines in thallus; (H), thallus and involucres; (I–K), spore clusters with pseudoelaters; (L), central columella with associated pseudoelaters and spores; (M–N), horn fragments with possible slit–like remnants of stomates; (O–P), thallus broken to show ensheathed nostocalean symbionts and rhizoids below; (Q) unensheathed nostocalean filament with heterocyst; (R–T), spores; (U–V), rhizoids on lower thallus. Specimens are PB2254 (A–E, H), PB2263 (F–G). Specimen J is on SEM stub UOF123865, K on stub UOF123864, and L, O–P, and V are on stub UOF123868. Specimens I, M–L, R–T are in slide UOF123854 at England Finder coordinates U40/4 (I), M52/2 (M), H43/2 (N), O35/2 (L), K47/3 (R), H47/4 (S), L19/3 (T) and J34/3 (U).

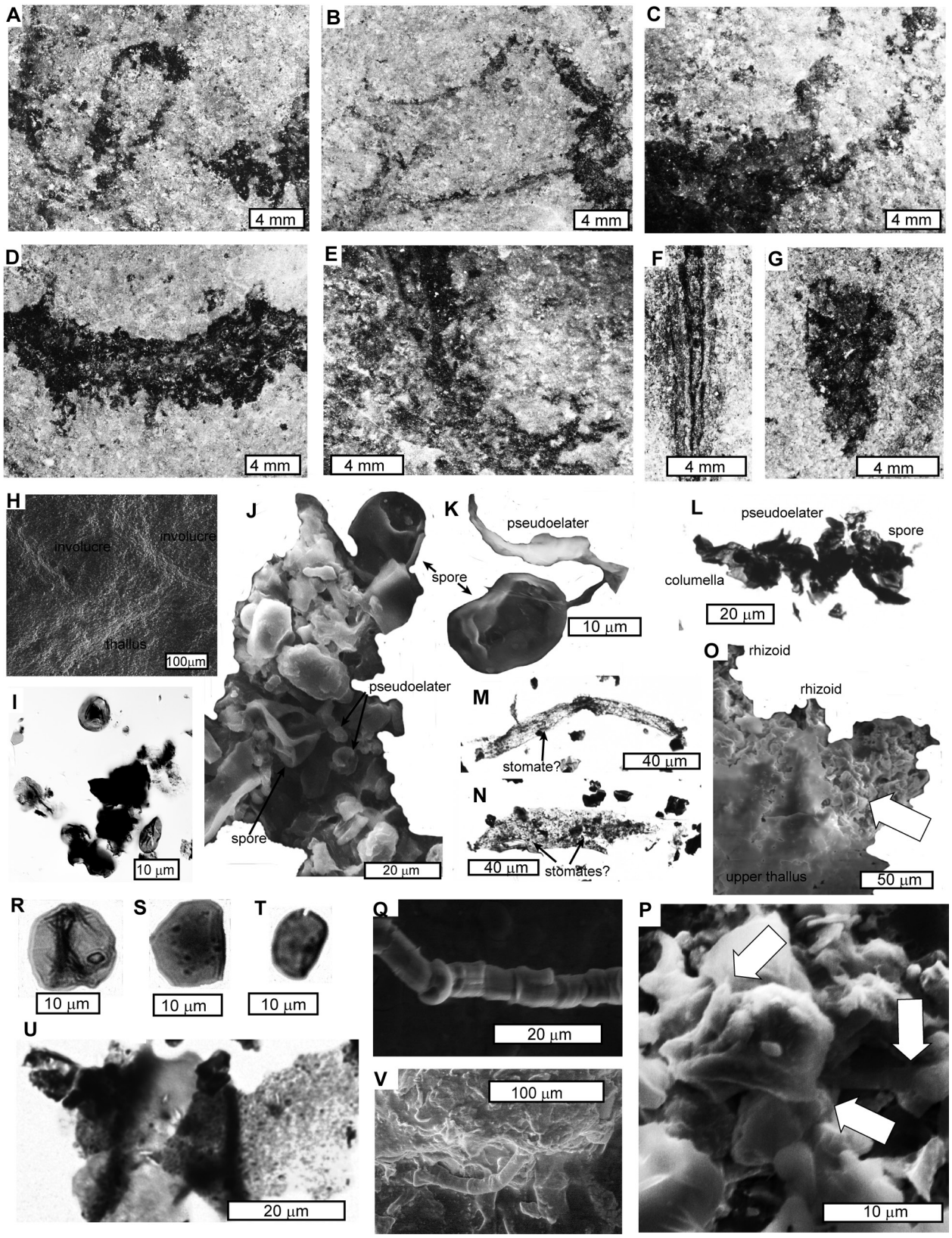
A
4 mm
B
4 mm
C
4 mm
D
4 mm
E
4 mm
F
4 mm
G
4 mm
H
involucre
involucre
thallus
100μm
I
10 μm
J
pseudoelater
spore
20 μm
K
pseudoelater
spore
10 μm
L
pseudoelater
spore
columella
20 μm
M
stomate?
40 μm
N
40 μm
stomates?
O
rhizoid
rhizoid
upper thallus
50 μm
R
10 μm
S
10 μm
T
10 μm
U
20 μm
Q
20 μm
V
100 μm
P
10 μm

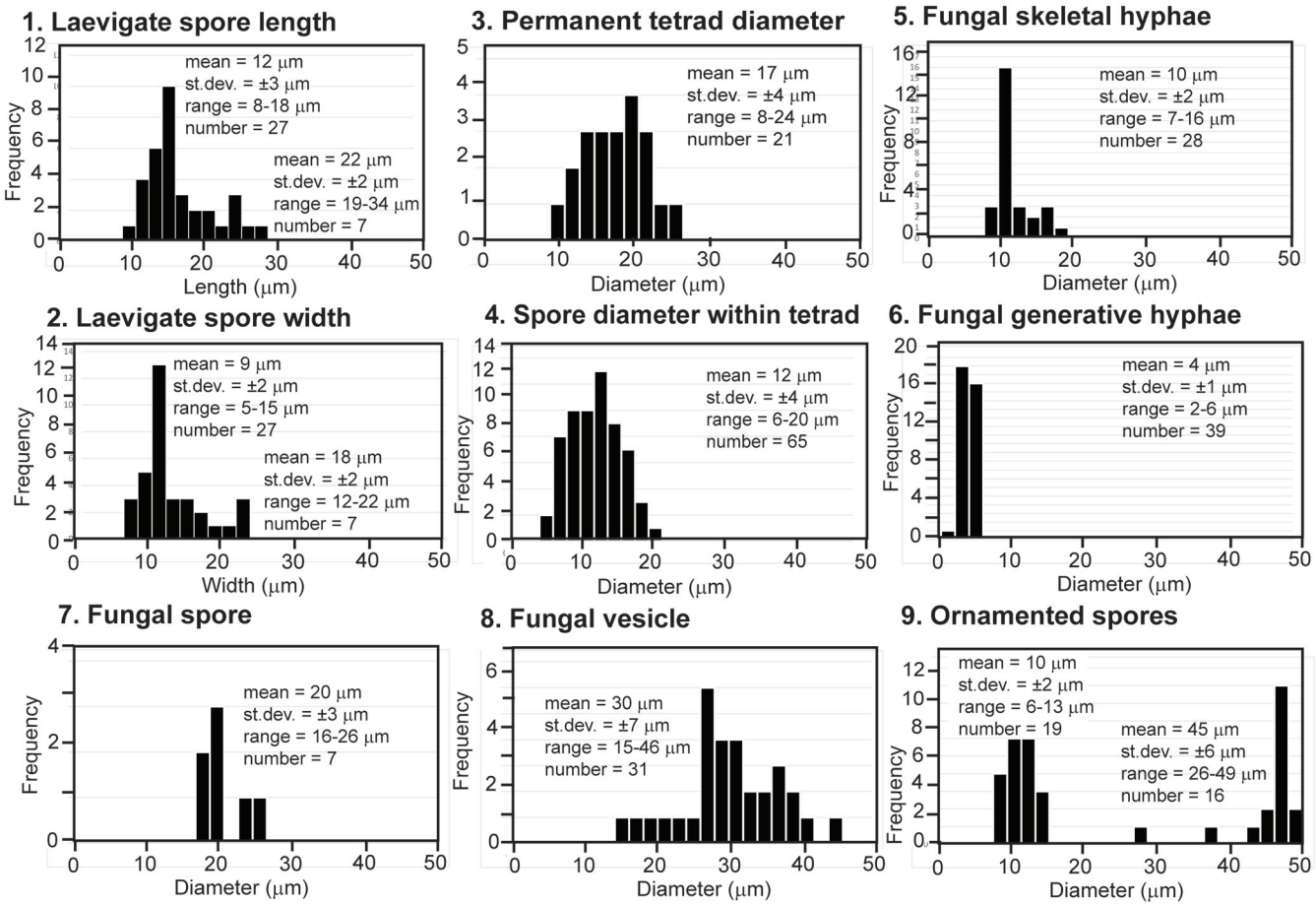

Fig. 7—Sizes of microfossils from the Middle Ordovician (Darriwilian) Douglas Dam Member, Tennessee (raw measurements in Table 1). Laevigate spores (1–2) are small from *Casterlorum crispum* new genus and species and large from *Dollyphyton boucotii* new genus and species. Tetrads (3–4) are from *Janegraya sibylla* new genus and species. Fungal skeletal and generative hyphae (5–6) are from *Prototaxites honeggeri* new species. Fungal spores and vesicles (7–8) are from *Palaeoglomus strotheri* new species. Ornamented spores (9) are small from *Edwardsiphyton ovatum* new spcies and large from *Cestites mirabilis* Caster and Brooks (1956).

is correlation with thick tuffs in Argentina (Huff *et al*., 1997, 2010) now dated at 470 Ma (Thompson *et al.,* 2012). The Precordillera Terrane of Argentina has Cambrian olenellid and ptychagnostid trilobites of Laurentian affinities and thick Early Ordovician carbonates like those of Tennessee (Thomas & Astini, 2003), so was not far distant at the time.

Ripple marks in plant–bearing silty dolostone (Fig. 2B–C) are evidence of mild current flow in shallow water. Shallow desiccation cracks (Fig. 2D), also noted by Laurence (1944), are evidence of exposure and drying. The plant–bearing layers also have shallow organic rooting structures (Fig. 2D, 2F) and arthropod tracks with push–up mounds as evidence of terrestrial weight–bearing motion (Fig. 2G–H). These features mark these layers with plant and arthropod fossils as very weakly developed paleosols, such as Fluvents (Retallack, 2001a). Many of the fossil plants appear to be in growth position, rather than transported, thus ruling out original interpretation as redeposited algae (Gray, 1988; Retallack, 2000). Oversized clasts of dolostone may have fallen into the varved shales and very weakly developed paleosols from sinkhole walls (Fig. 2E). Thus the fossil plants and amphibious arthropods are preserved within a sinkhole lake–margin terrestrial habitat.

Other clues to paleoenvironment of the Douglas Dam Lagerstätte come from articulated enigmatic arthropods (Caster & Brooks, 1956), the possible xiphosure *Chasmataspis laurenci* (Fig. 3C–D) and possible phyllocarid *Douglasiocaris collinsi* (Fig. 3E–F). *Douglasiocaris* has divergent cercopods, and the streamlined shape of an obligate aquatic creature, but *Chasmataspis* has mainly walking legs, and may have been amphibious. This is supported by discovery of simple trackways of *Diplichnites gouldi* (Fig. 2G–H, 3A–B) of comparable width to carriage of *Chasmataspis*, although tracks of this kind have also been attributed to millipedes and euthycarcinoids (Bradshaw, 1981; Retallack, 2009).

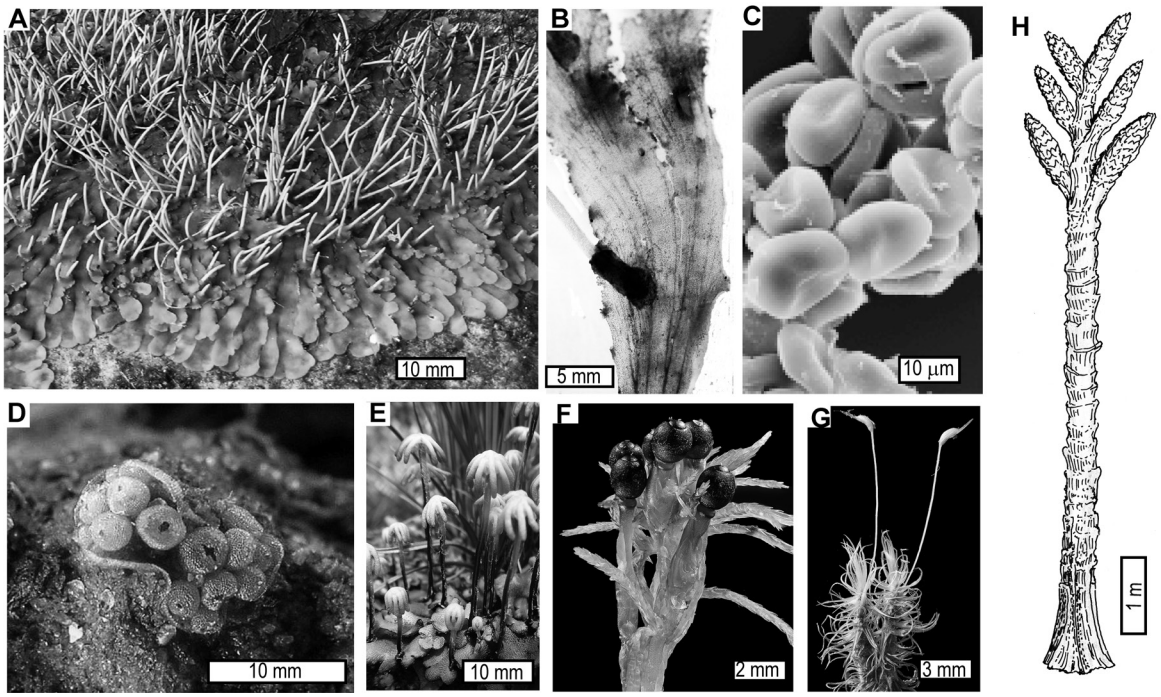

Fig. 8—Comparable modern and Devonian plants: (A–C), hornwort *Leiosporoceros dussi* from El Valle de Antón, Panama (courtesy of Juan Carlos Villareal); (D), balloonwort *Sphaerocarpos michelii* from Veltem–Beisem, Belgium (courtesy J. De Laet); (E), thalloid liverwort *Marchantia polymorpha*, Wanaka, New Zealand (courtesy P. Bendle); (F), moss *Sphagnum fimbriatum,* Lake Placid, New York (courtesy of Northern Forest Atlas): (G), *Dicranum ontariense*, Lake Placid, New York (courtesy of Northern Forest Atlas); (H), reconstructed tree–size lichen *Prototaxites loganii* from Devonian Bellvale Sandstone near Monroe, New York (Retallack & Landing 2014).

The Douglas Dam paleokarst may have been a deep freshwater sinkhole, comparable with modern cenotes of Yucatan (Laurence, 1944; Gray, 1988; Retallack, 2000). Like modern Ik Kil Cenote in Yucatan (Perry *et al.*, 2009), commonly included on the mass tourism itinerary to Chichen Itza, the Douglas Dam sinkhole may have been well lit by the sun to its base, and included both a lake and marginal muddy to rubbly shore. An alternative interpretation is a marine terrace near a freshwater spring, like those seen on the Florida Coast today (Caster & Brooks, 1956). This view is no longer tenable as there is no trace of marine fossils in the assemblage, and the ctenophore affinities of *Cestites* (Caster & Brooks, 1956) cannot be sustained by comparison with genuine fossil ctenophores (Conway Morris & Collins, 1996; Hou *et al*., 2017). Another alternative of "a lagoonal marginal marine setting" (Dunlop *et al*., 2003) is also mistaken in identifying sediments above the Knox unconformity as Five Oaks Formation (Steinhauff & Walker, 1995). Rocks overlying the Knox disconformity are the Douglas Dam Member of the lowest Lenoir Formation (Bridge, 1955; Walker *et al*., 1992).

MATERIALS AND METHODS

When Caster & Brooks (1956) described two new species of arthropods from shales at the unconformity between Early and Middle Ordovician carbonates at Douglas Dam, Tennessee, they also figured without description a variety of carbonaceous compression fossils. Some of these were rediscovered in the historic Caster Collection in the Department of Geology of the University of Cincinnati on June 17, 2016. The specimens were uncatalogued, but informative material has since been catalogued in collections of the Cincinnati Museum Center. The rest of the collection was discovered in the arthropod type room of the Smithsonian Institution, Natural History Museum, on August 13, 2016. Other material was collected in float from Douglas Dam during July 2016 fieldwork for this project, but its provenance is uncertain. The prospects of obtaining material additional to studied museum collections are thus very low.

Plant fossils from Douglas Dam are preserved as carbonaceous compressions in rocks that are not metamorphically altered, but thermally mature (Epstein *et al.*, 1977). Maceration of matrix samples in HF and Schultz solution yielded abundant mesofossil fragments, isolated spores, and hyphae. Walton transfers (Cridland & Williams, 1966) were made by coating with Hillquist Part A and B epoxy, then dissolution of rock in HF, and maceration in Schulz solution. Schultz maceration was usually harsh on these brittle compressions. An FEI QANTA environmental scanning electron microscope was used to examine spores within uncoated megafossils in both secondary and back–scatter mode.

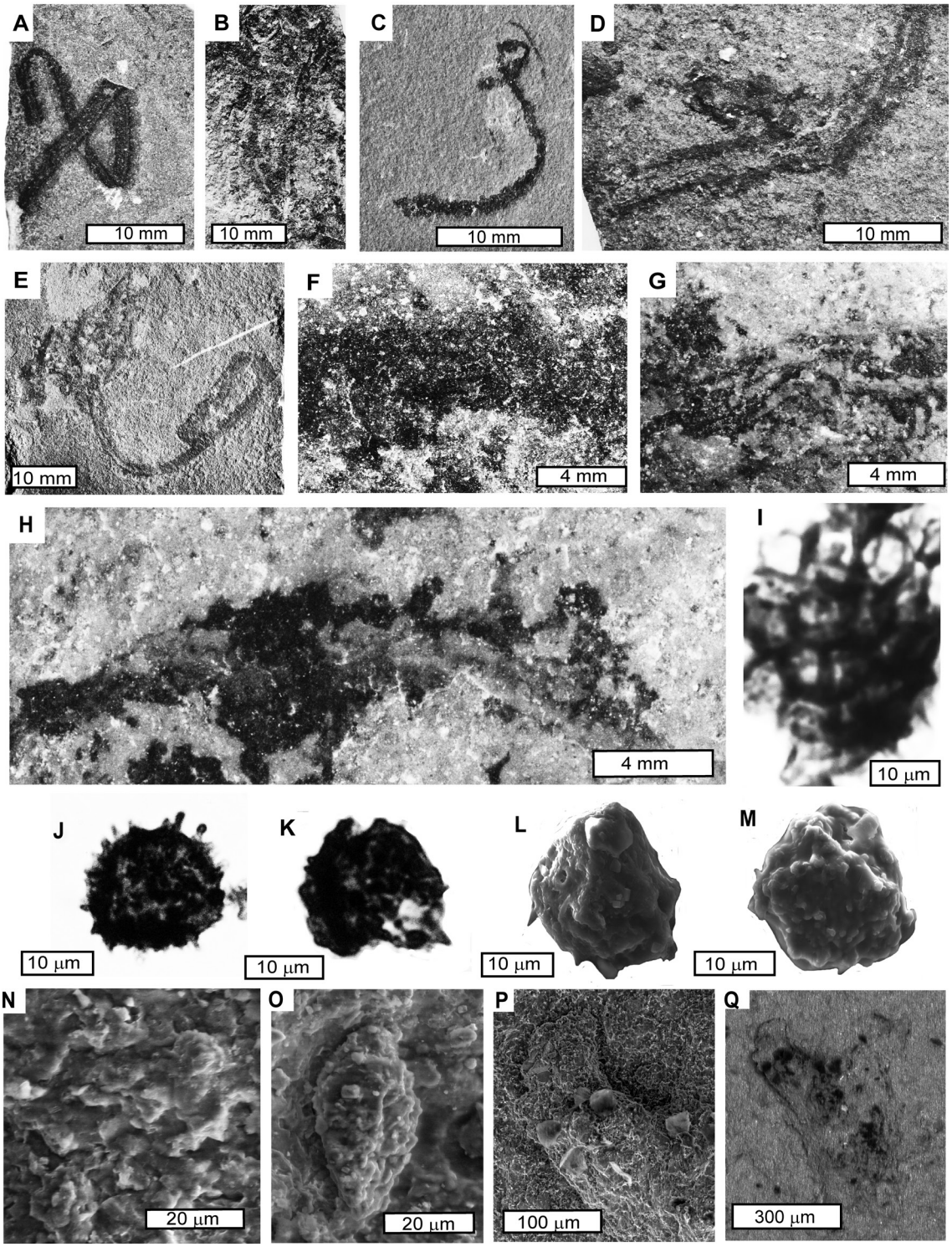

Fig. 9—*Cestites mirabilis* Caster & Brooks 1956, from the Middle Ordovician (Darriwilian) Douglas Dam Member, Tennessee; (A), holotype folded thallus; (B), dichotomising thallus; (C), folded thallus; (D), dichotomising thallus; (E), thallus with attached archegoniophores; (F–G), details of thalli with ventral scales; (H), thallus with ventral scales and archegoniophores; (I), arenchymatous tissue; (J–O), spores; (P–Q), archegoniophore. Specimens are USNM125087 (A), USNM125106 (B), USNM645562 (C); USNM645561 (D), PB2266A (E, G, N–O), PB2254 (F, H) and SEM stub UOF123867 (L–M). Unlike other secondary SEM images, panel 19 is back scatter with black carbon and gray phyllosilicate. Specimens J–K are in slide UOF123854 at England Finder coordinates R45/2 (I), T15/4 (J), T16/3 (K).

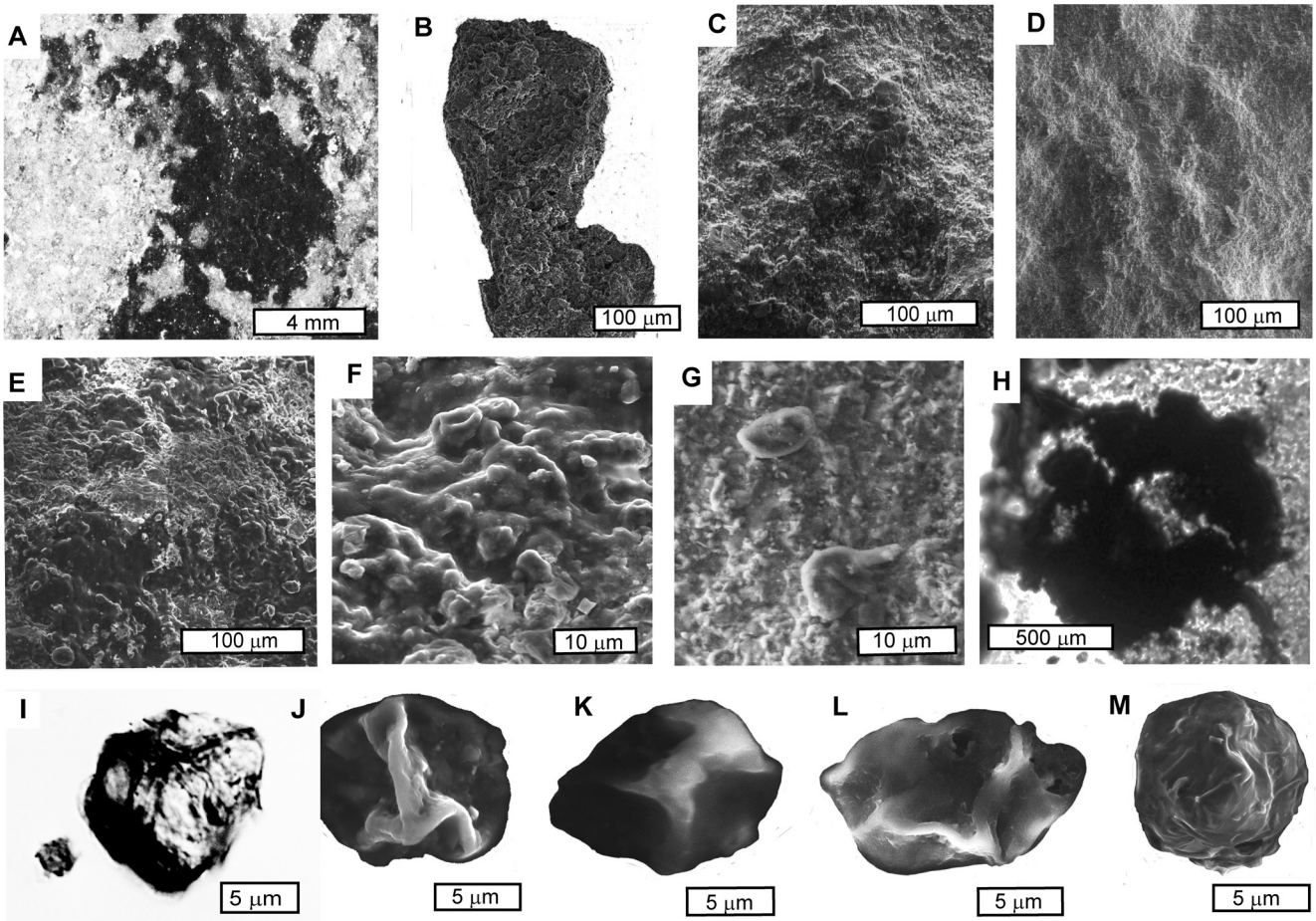

Fig. 10—*Janegraya sibylla* new genus and species from the Middle Ordovician (Darriwilian) Douglas Dam Member, Tennessee; (A), fertile thallus (holotype); (B–E), sporangia with pseudoperianth; (F–G), spore tetrads in rock; (H), pseudoperianth in transfer; (I–L), macerated spore tetrads; (M), spore tetrad in perine. Specimens are PB2254 (A, C–D, G), PB2283 (E–F), transfers UOF124275 (B) and UOF124280 (H), SEM stub UO123864 (J, L–M), and stub UOF123867 (K). Specimen I is in slide OUF123854 at England Finder coordinates C39/1.

Repository and institutional abbreviations—Material studied is in four institutions: U. S. Natural History Museum, Smithsonian Institution (prefix USNM–, 68 specimens including holotypes of *Chasmataspis*, *Douglasiocaris*, and *Cestites*, as well as many plants), Cincinnati Museum Center Paleobotany Collection (prefix PB–, 12 specimens of *Chasmataspis* and 38 specimens of fossil plants), University of Cincinnati (42 uncataloged specimens of rocks and fossils) and Condon Collection of the Museum of Natural and Cultural History of the University of Oregon (prefix OUF–, 35 specimens and 11 preparations of marine fossils and fossil plants).

SYSTEMATIC PALEONTOLOGY

Five taxa of the main clades of non–vascular land plants (Morris *et al.*, 2018; Puttick *et al.*, 2018) and two problematic fungal taxa (Redecker *et al.*, 2000, 2002; Retallack & Landing, 2014) are described here. These are paleobotanical taxa under provision of the International Botanical Code (Turland *et al.*, 2017). The following paragraphs are arranged by recent higher classifications (Hibbett *et al.*, 2007; Novikoff & Barabasz–Krasny, 2015). All raw measurements are tabled in Table 1.

Kingdom—Plantae Linnaeus, 1753

Division—Anthocerophyta Stotler & Crandall–Stotler, 1977

Class—Anthocerotopsida Janczkewski, 1872

Order—Leiosporocerotales Hässel de Menendez, 1988

Family—Leiosporocerotaceae Hässel de Menendez, 1986

Form genus—*Casterlorum* new genus

Figs 4A–B, 5, 6

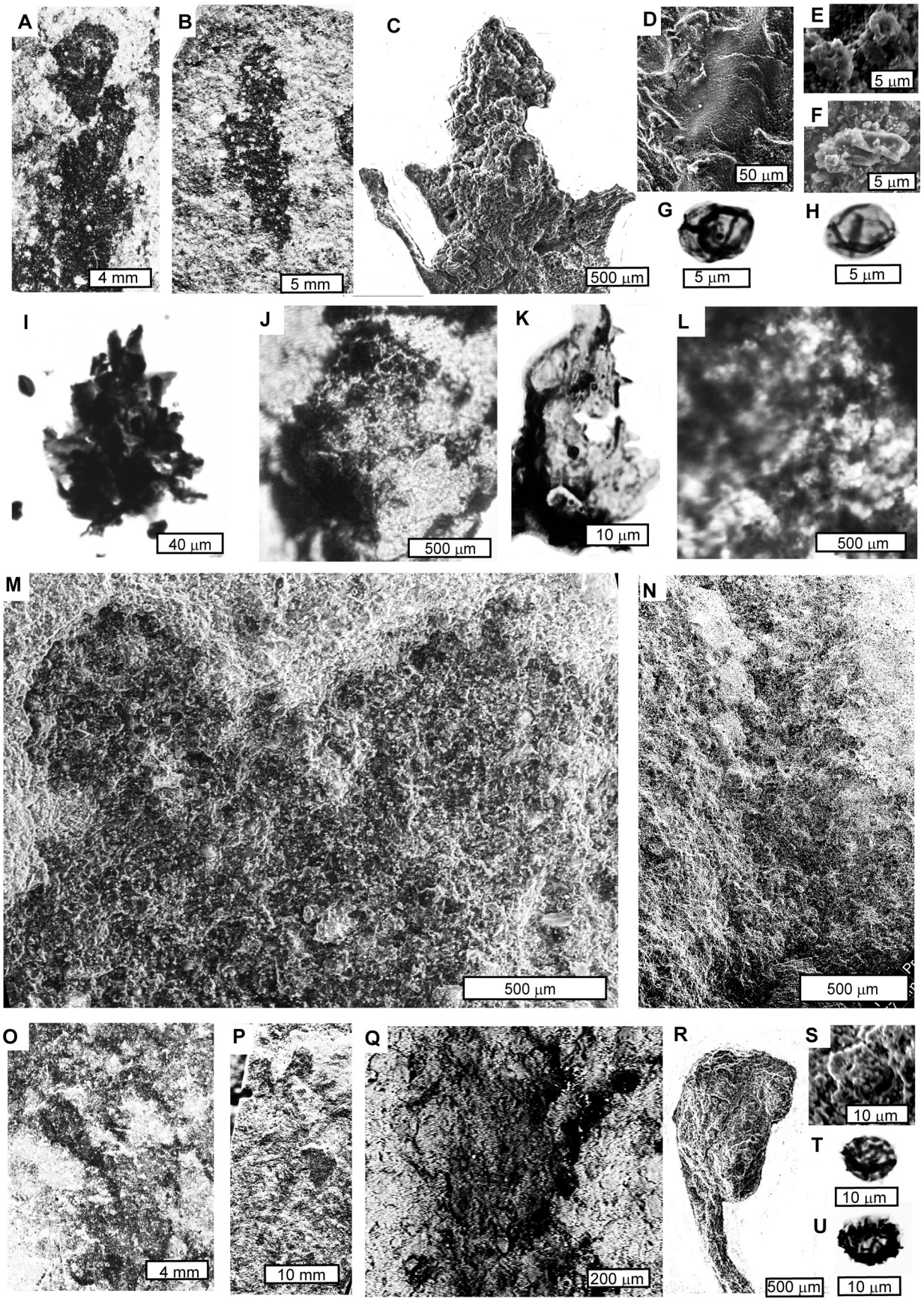
A
4 mm
B
5 mm
C
500 μm
D
50 μm
E
5 μm
F
5 μm
G
5 μm
H
5 μm
I
40 μm
J
500 μm
K
10 μm
L
500 μm
M
500 μm
N
500 μm
O
4 mm
P
10 mm
Q
200 μm
R
500 μm
S
10 μm
T
10 μm
U
10 μm

Type species—*Casterlorum crispum* new species

Diagnosis—Thallus prostrate and dichotomizing at intervals of 6 to 8 thallus widths; upper surface of thallus with dark grooves, dichotomizing apically, above channels with filamentous trichomes; long sporophytes on upper surface, with basal sheathing involucre and often curled and split outer portion; spores laevigate, ellipsoidal; pseudoelaters elongate and coiled.

Etymology—The generic name is compounded in honour of Kenneth Caster and the Latin *lorum* (whip).

Remarks—*Casterlorum* is similar in many respects, including cyanobacterial photosymbionts in bifurcating channels (Fig. 6F–G, O–P) and minute spores (Fig. 6J–K, R–T), to the living hornwort *Leiosporoceros dussii* (Hässel de Menendez, 1986; Villarreal & Renzaglia, 2006). Thus *Casterlorum* is attributed to the modern family Leiosporocerotaceae, considered basal among hornworts (Duff *et al*., 2007). *Casterlorum crispum* has narrower thalli, branches less frequently, and has longer and less tightly curled dehisced sporangia than *Leiosporoceros dussi* (Hässel de Menendez, 1986). Other living hornworts have distinctive large, heavily ornamented and trilete spores (Duff *et al*., 2007).

Devonian form genera *Sporogonites* (Andrews, 1960) and *Torticaulis* (Edwards *et al*., 1994) have elongate sporangia with columella–like central axis, much shorter and fusiform than in *Casterlorum*, and their thallus is virtually unknown. Among megafossil hornwort compressions of Cretaceous age, *Dendroceros victoriensis* (Drinnan & Chambers, 1986) and *Notothylacites filiformis* (Němejc & Pacltova, 1974) differ in their narrow thallus with clear midrib, unlike the multiple, bifurcating furrows of *Casterlorum*.

Casterlorum crispum new species

Figs 4A–B. 2, 5, 6

1956 Caster & Brooks, ‘carbonaceous films’ Pl. 23, figs 1–4.

Holotype—Individual thallus on a slab USNM125102 with 9 thalli and 28 horns, 6 cm past the number on slab in direction of green dot–sticker (Figs 4A, 5A).

Diagnosis—Thallus prostrate, 4.9 ± 1.6 mm wide (n=21), and dichotomizing at intervals of 6 to 8 thallus widths; upper surface of thallus with dark grooves, dichotomizing apically, above filamentous trichomes each 11.2 ± 1.7 μm long and 3.6 ± 0.3 μm wide (n=5); sporophytes abundant on upper surface, 0.9 ± 0.2 mm wide by 44 ± 16 mm long (n=15), with basal involucre 1.5 ± 0.3 mm wide by 6.4 ± 2.8 mm long (n=27); dehisced sporangia irregularly curled; sporophyte columella 7 ± 2 μm diameter (n=7); spores laevigate, ellipsoidal, and 12 ± 2 μm long by 9 ± 2 μm long (n=27); pseudoelaters 12 ± 4 μm long by 6 ± 1 μm wide (n=8).

Description—The most abundant fossils of Douglas Dam Member are diaphanous thalli with attached thick–carbonaceous horns that are sometimes split into deep curls (Figs 4B, 5E–H, 6A–C). The abundance and spacing of horns at an angle to the thallus are best appreciated from a specimen on the same slab and to the right of the holotype (Fig. 5A). The holotype is one of the nine individuals scattered in growth position over a large slab, and these vary considerably in thallus preservation from a wide thallus flange, to largely decayed thallus around a few thallial grooves. The slender horns include a thick carbonized basal sheath identified as an involucre (Figs 4A–B, 5A–C, 6A–C, H), and these persisted on many coiled horns after thallus remnants decayed (Figs 4B, 5E–H). These remains are all black with organic matter, and lack the shiny surfaces of associated arthropods (Fig. 3C–F), and the clayey fill of rooting and burrowing structures (Fig. 2D, F). The thallus has dark grooves (Figs 4A, 5A, C–D, 6E–F) which form a distinctive open dichotomous pattern (Fig. 6E–F) that becomes reticulate at the apex (Figs 5C, 6G). Shattered thalli revealing histology beneath the grooves have elongate, sheated and bare, multicellular filaments including larger cells like heterocystous cyanobacteria (Fig. 6O–Q). Thus the dark grooves on compressions are interpreted as mucilage channels for photosymbionts. Horn fragments show elongate cells and imperfectly preserved slits that might be stomates (Fig. 6M–N). No likely stomatal openings were seen on the thalli (Fig. 6O, U). Rhizoids are visible on the lower side of partly decayed thalli (Figs 6D, U–V).

Spore clusters are associated with elongate carbonized columella remnants and pseudoelaters (Fig. 6J–K). Spores of *Casterlorum* are laevigate, small and ellipsoidal, unlike a less common larger and more spherical population of associated laevigate spores attributed here to *Dollyphyton* (Fig. 7A–B).

Etymology—The epithet *crispum*, Latin for curly, refers to dehisced sporangia.

Materials—Slabs PB2251, PB2252, PB2254, PB2263, USNM125104, USNM128086, USNM128088–92, and USNM645551–9. A 20 g fragment with thalli from PB2254 was dissolved in HF and macerated in Schulz solution to reveal

Fig. 11—*Dollyphyton boucotii* new genus and species (A–M) and *Edwardsiphyton ovatum* gen. et sp. nov. (N–U) from the Middle Ordovician (Darriwilian) Douglas Dam Member, Tennessee; (A–C), shoots with terminal capsule (holotype = B); (D), leaves; (E–H), spores;(I), small–leaved shoot; (J–K), large leaves; (L) leaf cuticle: (M–N), leafy shoots; (O–P), shoots with reflexed capsules (holotype =N); (Q), leaves, black in back scatter SEM; (R), capsule; (S–U), spores. Specimens are PB2275 (A, F, M, N), USNM645801 (B), PB2266 (O), and PB2281 (P–Q). Transfers are UOF124275 (C, E), UOF124280 (D, J, L), UOF124276 (R–S). Others are from slide OU123854 at England Finder coordinates L38/4 (G), W17/4 (H), J60/1 (I), V30/2 (K), S49/2 (T) and T49/1 (U).

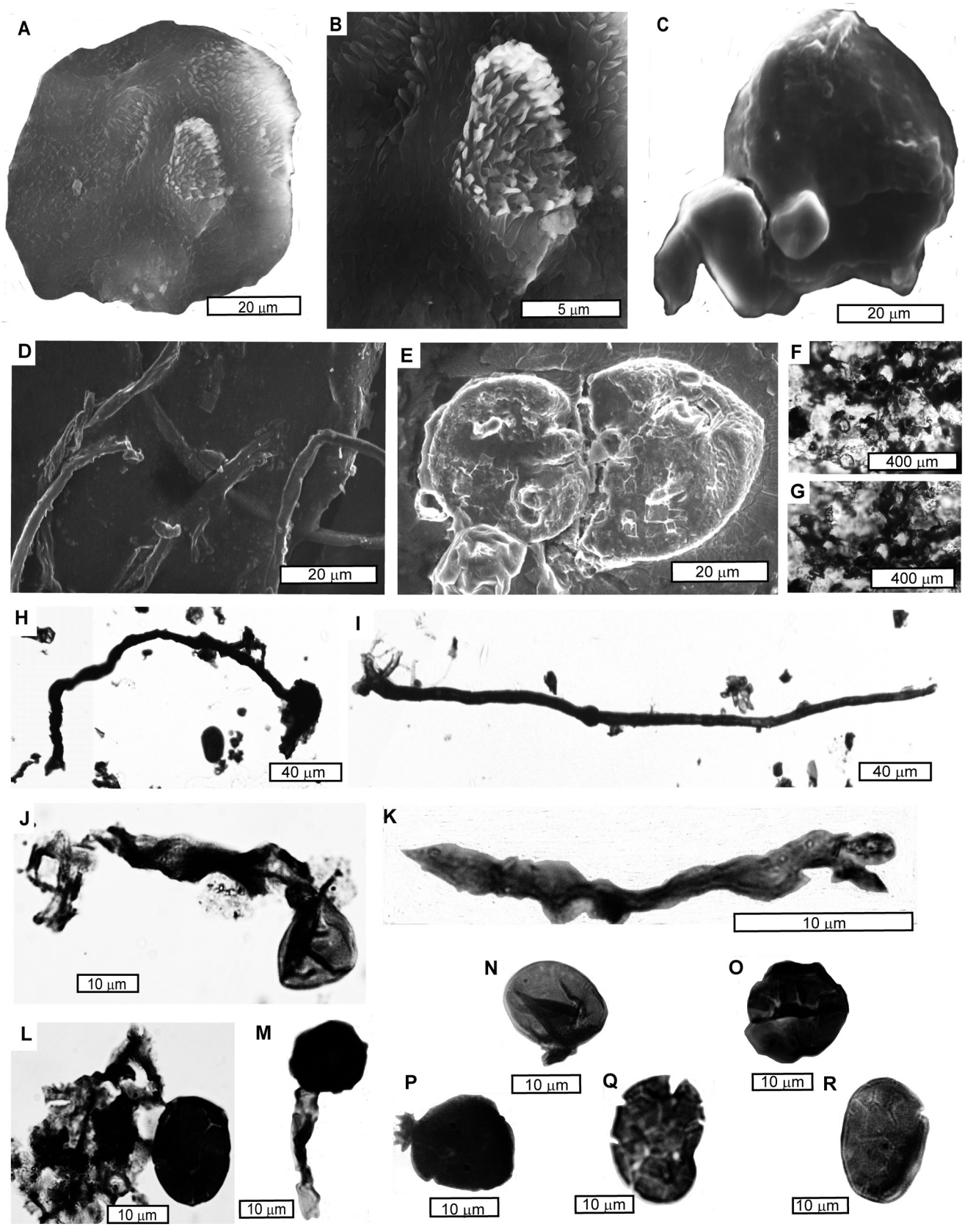
A
20 μm
B
5 μm
C
20 μm
D
20 μm
E
20 μm
F
400 μm
G
400 μm
H
40 μm
I
40 μm
J
10 μm
K
10 μm
L
10 μm
M
10 μm
N
10 μm
O
10 μm
P
10 μm
Q
10 μm
R
10 μm

clusters of spores with associated columella and pseudoeaters in slide UOF123854, and SEM stubs UOF123865 and UOF123868. Thalli of *Casterlorum* proved too fragile for successful transfer and maceration.

Remarks—Multicellular filaments within the thallus are similar to cyanobacteria, but not like *Nostoc* or *Anabaena*. Their pill–shaped cells (Fig. 6O) and thick sheaths (Fig. 6P) are more like *Oscillatoria* or *Scytonema* (Zapomělová *et al*., 2008). Some larger cells in the filaments may have been heterocysts, and an indication of nitrogen fixation (Tyagi, 1975).

Spores of *Casterlorum* do not appear to have been named in the formal taxonomy of dispersed spores and are somewhat more variable than dispersed spore species (Steemans & Wellman, 2018). They are small and smooth like *Spissuspora laevigata* (Steemans & Wellman, 2018), but unlike that species are not spherical and show some contact modifications. Unlike *Imperfectotriletes* (Steemans & Wellman, 2018), the Tennessee spores are small and lack tears. Similar elongate clusters of small spores like those of *Casterlorum crispum* from Middle Ordovician rocks of Saudi Arabia have been designated informally "densely packed, laevigate sphaeromorphs" (Le Hérissé *et al*., 2017).

Casterlorum crispum may have been a hornwort similar to living *Leiosporoceros dussi* (Fig. 8A–C: Hässel de Menendez, 1986; Villarreal & Renzaglia, 2006), and thus the geologically oldest known fossil representative of hornworts (Oostendorp, 1987; Pant & Bhowmik, 1998). The molecular phylogenetic position of hornworts within bryophytes is uncertain with seven viable alternatives (Morris *et al*., 2018), but one currently favoured is hornworts basal to a monophyletic bryophyte clade as a sister group to tracheophytes (Puttick *et al.*, 2018).

Phylum—Marchantiophyta Crandall–Stotler & Stotler, 2000

Class—Marchantiopsida Cronquist *et al*., 1966

Order—Marchantiales Limpricht, 1876

Family—Marchantiaceae Lindley, 1836

Form genus—*Cestites* Caster & Brooks, 1956

Type species—*Cestites mirabilis* Caster & Brooks, 1956

Cestites mirabilis Caster & Brooks, 1956

Figs 4G, 9

1956 Caster & Brooks *Cestites mirabilis* Pl. 23, fig. 5.

Holotype—USNM125087 (Fig. 9A).

Revised diagnosis—Thallus prostrate, 3.2 ± 1.0 mm wide (n=13), and dichotomizing at intervals of more than 12 thallus widths; upper surface of thallus with multistranded midrib, 1.6 ± 0.6 mm wide (n=13), and orthogonally undulose flanks; archegoniophore disks peltate, 4.4 ± 1.4 mm wide (n=14) on long (8.5 ± 2.3 mm, n=7) stalks 0.9 ± 0.2 mm (n=8) wide; spores 46 ±7 μm diameter (n=16), subtriangular, strongly ornamented with pseudotrilete ridge and prominent verrucae and bacculae; ventral narrow acute–tipped scales 55 ± 14 μm long (n=5) by 31 ± 8 μm wide (n=5); multicellular rhizoids 20 ± 5 μm diameter (n=7).

Description—*Cestites mirabilis* was originally described by Caster & Brooks (1956) as a comb of a ctenophore, but the holotype is folded over like a noodle (Fig. 9A), very different from stiff, parallel, combs of genuine fossil ctenophores, for example, those of Cambrian shales near Chengjiang, China (Hou *et al*., 2017), and Field, British Columbia (Conway Morris & Collins, 1996). Newly discovered specimens of *Cestites mirabilis* show dichotomies at long intervals like a liverwort or alga (Fig. 9B–C). Two specimens are encountered with many attached parasol like structures, hence interpreted as archegoniophores. (Figs 4G, 9E, H). These are unusually crowded on the thallus, with attachment evident only in a few. These archegoniophores may be an accidental tangle, because the thallus is bent in a manner suggesting transport. Other specimens show other liverwort features (Crandall–Stotler *et al*., 2009), such as aerenchymatous tissue (Fig. 9I), acutely tipped ventral scales (lower left of Fig. 9H), and rhizoids (Fig. 9F–G). Preservation ranges from complete (Fig. 9A–E) to partly decayed thallus (Fig. 9F–G). The mature archegoniophores are peltate with 10–12 reflexed lobes (Fig. 4G, 9F). Small putative archegoniophores lack lobes and terminate in apical hollows (Fig. 9H, P–Q). Back scatter electron microscopy shows that these unlobed structures have dense carbonaceous masses (Fig. 9Q), perhaps immature sporangia.

Scanning electron microscopy of a fertile specimen revealed a sporangium full of highly ornamented, baculate to verrucate, spores (Fig. 9N–O), that also are common in the matrix (Fig. 9J–M). At least two taxa of similar spores are represented in the Douglas Dam Assemblage based

Fig. 12—*Palaeoglomus strotheri* new species from the Middle Ordovician (Darriwilian) Douglas Dam Member, Tennessee; (A–B), vesicle with echinate ornament on lobes (holotype); (C), vesicle and hypha;(D), hyphae; (E), vesicles; (F–G), vesicles and arbuscles; (H–O), vesicles on hyphae; (Q–R), spores. Specimens are on SEM stub UOF123864 (A–B, D–E) and UOF1233867 (C), transfer UOF124277 (F–G) and slide OUF123854 (H–R) at England Finder coordinates F38/1(H), V38/1(I), T16/3(J), F38/3(K), L39/1(L), K16/3(M), F48/3(N), J47/4(O), S45/2(P),L38/3(Q), and F14/2(R).

on ornament and size (Fig. 7I). One is small (10 ± 2 µm diameter, n=19) with curved muri, and the other is larger (40 ± 9 µm diameter, n=4) with verrucae. Only the large spores have been found in a sporangium of *Cestites*, and the small ornamented spores have been found in and around capsules of *Edwardsiphyton ovatum* gen. et sp. nov.

Materials—Slabs USNM125062, USNM645561, PB2266, PB2254. A 20 g fragment of PB2254 was dissolved in HF and macerated in Schultz solution to create the residue of slide UOF123854, SEM stubs UOF123867 and UOF123868, and part of a thallus on PB2266 was lifted as transfer UOF124277.

Remarks—Thalli of *Cestites* are distinct from those of *Casterlorum*, in their wide furrowed midrib (Figs 4G, 9A–H), rather than dichotomizing near–parallel dark channels (Figs 5A, 6E–G). When horns are present on *Casterlorum* the distinction is even more obvious. *Cestites mirabilis* is similar to palaeobotanical form genera for thalloid liverworts ranging back to Devonian in age, such as *Hepaticites* (Hueber, 1961), *Marchantites* (Li *et al.*, 2014), *Marchantiolites* (Brown & Robinson, 1976), *Metzgeriothallus* (Hernick *et al*., 2008), *Ricciopsis* (Hoffman & Stockey, 1997), and *Pallaviciinites* (Li *et al*., 2016), but *Cestites* differs from these because of its wide midrib occupying a third of the thallus width, and its sparse dichotomies. *Riccardiothallus* (Guo *et al*., 2012) is different again, because its thallus lacks a clear midrib, and branches irregularly. Fragmentary peltate structures from the Late Ordovician of Poland (Salamon *et al*., 2018) resemble archegoniophores of *Cestites*. Thalli and lobed archegoniophores of *Cestites mirabilis* are similar to those of living *Marchantia polymorpha* (Fig. 8E).

Ornamented spores like those of *Cestites mirabilis* in Ordovician rocks elsewhere have been referred to un–named species of the dispersed spore genus *Hispanaediscus* (Rubinstein & Vaccari, 2004; Vecoli *et al*., 2011) and "monad with rounded verrucae" (Vecoli *et al*., 2017). Spores of *Cestites* also have a strong resemblance to spores of living *Marchantia berteroana* (Taylor *et al.*, 1974).

Order—Sphaerocarpales Cavers, 1910

Family—Sphaerocarpaceae Heeg, 1891

Form genus—*Janegraya* new genus

Type species—*Janegraya sibylla* new species

Diagnosis—Thallus small and discoidal, covered in barrel–shaped pseudoperianths with two levels of obovate leaves; spores permanently united in tetrads within thin, wrinkled, envelope.

Etymology—The generic name is in honour of Jane Gray, who predicted such a plant from its spores.

Remarks—These small discoid compressions with sporangia of permanent tetrads fulfill a prediction of Gray (1985) that dispersed permanent tetrads of *Tetrahedraletes* were produced by a plant similar to the living balloonwort, also known as a bottle liverwort, *Sphaerocarpos* (Haynes, 1910). The most similar modern species to *Janegraya sibylla* is the balloonwort *Sphaerocarpos hians*, but all modern *Sphaerocarpos* spores are much larger and have a coarse mesh of folds on the perine surrounding the permanent tetrad (Haynes, 1910). Living *Sphaerocarpos* also differ in having pseudoperianths that are contracted at the apex or with a very narrow base (Fig. 8.4), whereas those of *Janegraya* are stout, more numerous, sessile, and open at the apex. The Triassic bottle liverwort *Naiadita lanceolata* differs from both *Janegraya* and *Sphaerocarpos* in having a longer axis with well–spaced, helically arranged lanceolate leaves, and was until now, the oldest known balloonwort (Hemsley, 1989).

Janegraya sibylla new species

Figs 4H, 10

Holotype—Slab PB2254 (Figs 4H, 10A).

Diagnosis—Thallus discoidal, 2.4–3.2 mm diameter (n=4), covered in 20–30 barrel–shaped pseudoperianths with two levels of obovate leaves, 434 ± 39 µm long (n=10) by 380 ± 51 µm diameter (n=16); sporangium elliptical 103 ± 16 µm diameter (n=22); spores permanently united in tetrads within thin, wrinkled, envelope, and 17 ± 4 µm diameter (n=17); individual spores within the tetrads 12 ± 4 µm diameter (n=65).

Description—These are inconspicuous discoidal thalli, only 2.4–3.2 mm in diameter. The holotype thallus is covered in 24 barrel–shaped pseudoperianths, but with an additional 26 pseudoperianths and sporangia scattered nearby in the matrix (Figs 4H, 10A), perhaps from other thalli. Both transfers (Fig. 10B, H) lost most of the thallus to acid maceration, but the spore masses did not clear to transparency in transmitted light (Fig. 10H). Thus the thallus is delicate and probably only one cell thick. The thallus may also have been rotting when the plant developed spores. Six pseudoperianth elements are each lobate (Fig. 10B–E), but the pseudoperianth is not strongly constricted at the base (Fig. 10B).

Spore masses of sporangia are scattered in the sediment, both within (Fig. 10B–D) and unenclosed by pseudoperianth (Fig. 10E). Permanent spore tetrads are in dense clusters (Fig. 10E–F), or separated in matrix (Fig. 10G). Spore tetrads vary in shape from equant (Fig. 10I–J) to elongate (Fig. 10K–L), and some are still enveloped in wrinkled perine (Fig. 10M). The tetrads are only a little larger than the spores within the tetrad (Fig. 7C–D).

Etymology—The epithet *sibylla* is Latin for prophetess.

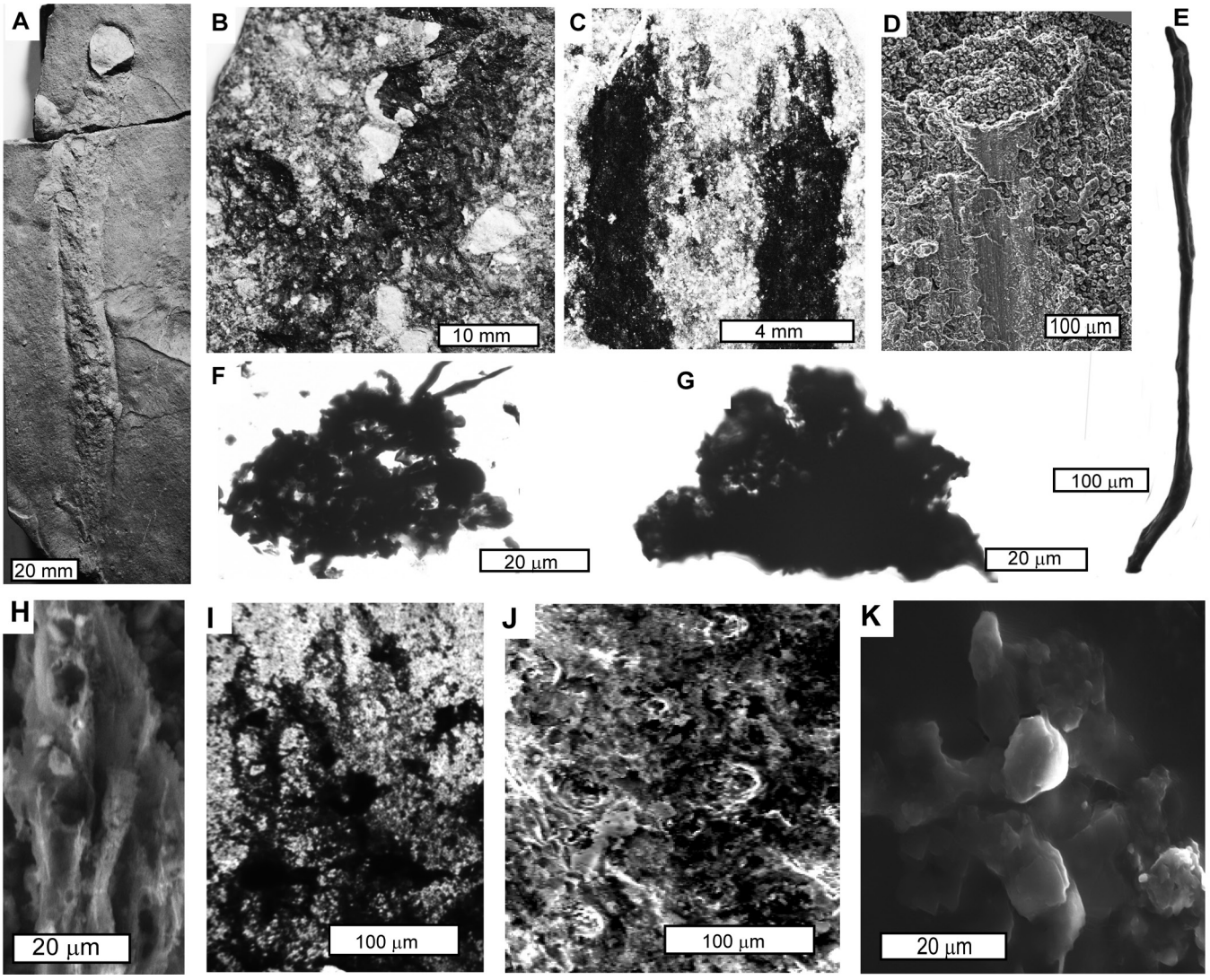

Fig. 13—*Prototaxites honeggeri* new species from the Middle Ordovician (Darriwilian) Douglas Dam Member, Tennessee; (A), trunk with branch scars; (B), branching apex (holotype); (C–D), palisades of skeletal hyphae around central hollow; (E), skeletal hyphae; (F–G), cortical nests within incurled generative hyphae and flanking skeletal hyphae; (H–J), vertical skeletal hyphae and curled generative hyphae in secondary SEM; (K), haustorial connections of generative hyphae to small spheroidal photobionts. Specimens are slabs USNM125083 (A), USNM125084=holotype (B), PB2277 (C,J), and PB2269 (H), and SEM stubs UOF123865 (E), OUF123868 (K), transfer UOF124279 (D, I), and slide OUF123854 at England Finder coordinates T22/2 (F), and V31/2 (G).

Materials—Specimens are slabs PB2283 and PB2254, with the latter also used for transfer UOF124275, and macerated for SEM stubs UO123864 and UOF123867.

Remarks—Permanent spore tetrads of *Janegraya* agree broadly with the dispersed spore taxon *Tetrahedraletes grayae* (Steemans & Wellman, 2018), but are about half the size (Strother, 1991), and similar to un–named tetrads in an isolated Early Ordovician (Floian) sporangium (Wellman *et al.*, 2003). They may be a new species, but are more variable than a dispersed spore species (Fig. 10I–M).

Division—Bryophyta Braun, 1864

Class—Sphagnopsida Schimper, 1857

Order—Sphagnales Limpricht, 1876

?Family—Flatbergiaceae Shaw in Shaw *et al.*, 2010

Form genus—*Dollyphyton* new genus

Type species—*Dollyphyton boucotii* new species.

Diagnosis—Axis with helically arranged, ovate, multistratose leaves, with multiple unicellular sharp teeth on each side; short files of 3–4 hyaline cells surrounded by thin chlorophyllose cells; capsule erect, ellipsoidal, and terminal on a short pseudopodium, and with a clear operculum; spores laevigate, with irregular folds.

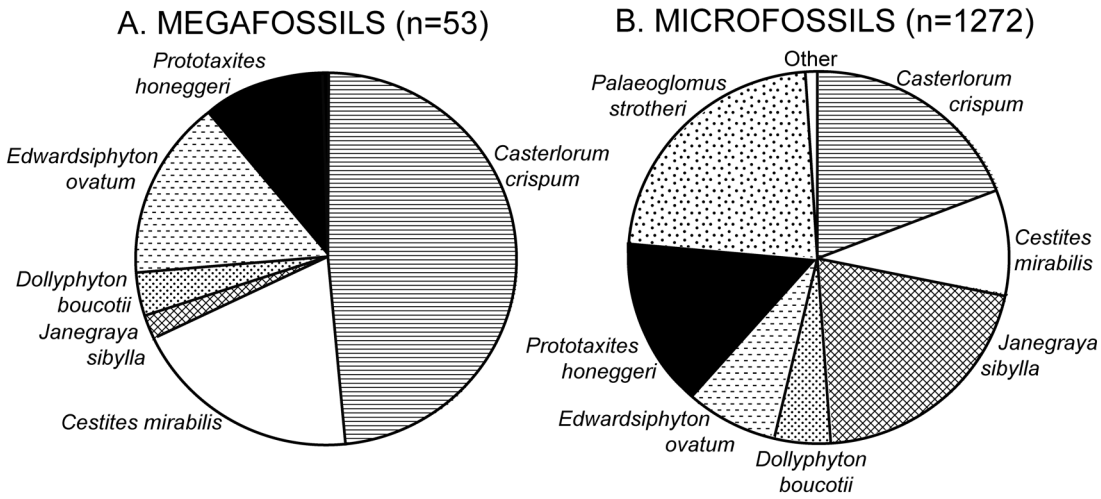

Fig. 14—Relative proportions of (A) megafossils and (B) microfossils from the Middle Ordovician (Darriwilian) Douglas Dam Member, Tennessee.

Etymology—The generic name is in honour of Dolly Parton, whose Dollywood resort is near Douglas Dam.

Remarks—The short pseudopodium and erect operculate capsule of *Dollyphyton* is similar to peat mosses (Sphagnales: Fig. 8F). Capsules and stem leaves of living *Flatbergium* (Sphagnales, Flatbergiaceae) are most similar to *Dollyphyton*, but their leaves are mucronate (Shaw *et al*., 2010). Like *Flatbergium*, *Dollyphyton* may have had minute branch leaves as well (Fig. 11I), but these remains have not yet been found attached, so there remains doubt about the family assignment. Spores of living peat mosses are quite different: strongly trilete with sulci between laesurae on a somewhat flattened proximal face (Terasmae, 1955; Brown *et al*., 1982; McQueen, 1985; Brubaker *et al*., 1998).

Another Ordovician (Sandbian) plant with helically inserted leaves is *Akdalophyton caradockii*, which has been macerated to reveal hydroids and stomates suggestive of moss affinities (Snigirevskaya *et al*., 1992). No capsules are known for *Akdalophyton*, and its leaves are narrow with rounded apices, unlike *Dollyphyton*. Close helical arrangement of leaves differentiates *Dollyphyton* from other Ordovician leafy axes such as *Hepaticaephyton* (Kozlowski & Greguss, 1959), *Musciphyton* (Greguss, 1962), and un–named forms (Retallack, 2001b, 2015a), which are comparable with living soil–interstitial, leafy–liverworts such as *Cephaloziella* (Schuster, 1956; Newsham, 2010). Sphagnalean leaf fragments of Ordovician age have more hyaline cells (7–8) in each file than seen in *Dollyphyton* (Cardona–Correa *et al*., 2016). Permian *Protosphagnum* and *Vorcutannularia* also differ from *Dollyphyton* in having clear midribs to the leaves (Neuburg, 1960). Triassic *Muscites* differs from *Dollyphyton* in narrow leaves and capsule with longitudinal dehiscence, like modern Andraeaceae (Anderson, 1976).

Dollyphyton boucotii new species

Figs 4F, 11A–M

Holotype—Slab PB2275 (Figs 4F, 11B, M).

Diagnosis—Axis with helically arranged, ovate, multistratose leaves, 4.4 ± 0.4 mm long by 1.7 ± 0.2 mm wide (n=7), with 9 sharp teeth on each side; capsule erect, ellipsoidal, 4.7 ± 0.7 mm long by 3.0 ± 0.3 mm wide (n=2), and terminal on a 1.6 ± 0.4 mm long (n=2), 0.3 ± 0.2 mm diameter, n=2) pseudopodium, with 1.8 ± 0.2 mm diameter (n=2) operculum; spores laevigate, 11 ± 1 μm diameter (n=7), with irregular folds.

Description—Two distinct kinds of slender axes with helically arranged leaves and terminal sporophytes are present: one referred to *Dollyphyton* with wide leaves and erect capsules on a short pseudopodium (Figs 4F, 11A–D, M), and a second referred to *Edwardsiphyton* with narrow leaves and recurved capsules on a long seta (Figs 4E, 11N–Q). The leaves of *Dollyphyton* are ovate, acutely pointed, multistratose, and wide at the base with 9 sharp teeth on either side (Fig. 11J–K, M). Cell outlines on the leaves are beaded in transfers under transmitted light, so may have been remains of chlorophyllose cells outlining hyaline cells (Fig. 11J–K). Openings on the large axial leaves are probably pores rather than stomates, because they have a guard–like cell on one side, but several cells on the other side (Fig. 11L). Minute leafy apices were also found (Fig. 11I), and may have been immature branches or polymorphic branch leaves, but these were not found attached. The terminal capsule is erect with a wide apical operculum, and constrictions near the base are indications of a pseudopodium, rather than a seta (Figs 4F, 11A–B).

Spores found in clusters within a partly decayed capsule (Fig. 11E–F) and loose in the rock (Fig. 11G–H) are laevigate

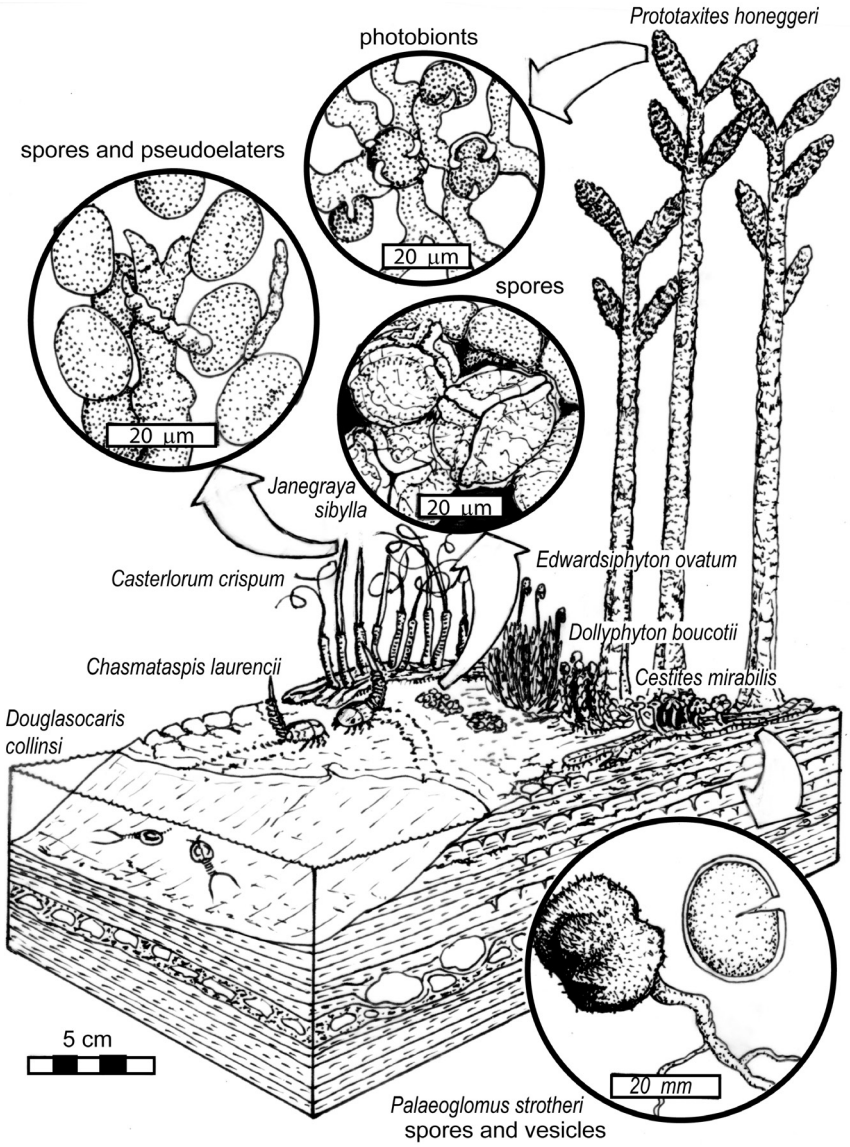

Fig. 15—Reconstruction of land plants and animals of the Middle Ordovician (Darriwilian) Douglas Dam Member, Tennessee.

like those found in *Casterlorum*, but larger (22 by 18 µm) and more spherical (Fig. 7A–B).

Etymology—The epithet honours Art Boucot, pioneer with Jane Gray in studies of early land plants.

Materials—Slabs PB2275 and USNM645801. Offcuts from slab PB2254 were used to make slide UOF123854, SEM stubs UOF123863–4, and UOF123867–8, and transfers UOF124375, UOF124280.

Remarks—Spores of *Dollyphyton* are generally similar to the dispersed spore genus *Imperfectotriletes* (Steemans & Wellman, 2018), but folds are seldom trilete in *Dollyphyton* (Fig. 11G–H). Dispersed spores of *Besselia* are also similar but finely verrucate and baculate (Nøhr–Hansen & Koppelhus, 1988). Spores of *Dollyphyton* are most like the Ordovician dispersed spore genus *Spissuspora* (Steemans & Wellman, 2018).

Class—Bryopsida Pax, 1900

Order—Pottiales Fleischer, 1920

?Family—Pottiaceae Schimper, 1843

Form genus—*Edwardsiphyton* new genus

Type species—*Edwardsiphyton ovatum* new species

Diagnosis—Axis with helically arranged, narrow acuminate, entire–margined, leaves, arched outwards from the axis; capsule ovate, reflexed, and on a long seta; peristome with 16 attenuate teeth, undivided transversely and longitudinally: spores small, ellipsoidal, and strongly ornamented with bacculae.

Etymology—The generic name honours Dianne Edwards, for work on early land plants.

Remarks—The single ring of 16 capsular teeth, which lack transverse lines (thus not arthrodont) and longitudinal divisions (thus not dicranoid), is most like the moss family Pottiaceae (Fig. 8G; Flowers, 1973), but assignment to that family must be regarded as provisional until better preserved material is discovered. Spores found in the capsule of *Edwardsiphyton* are also similar to those of the Pottiaceous moss *Tortula leucostoma* (Brubaker *et al*., 1998). Capsules as strongly reflexed as those of *Edwardsiphyton* are not known among extant Pottiaceae. Capsule drying can produce this effect in only moderately angled capsules of living *Timmia austriaca* (Timmiaceae: Flowers, 1973), but this reflexion is consistent in all 7 fossil capsules known, and may be a feature distinguishing the fossils from similar modern plants.

The narrow acute leaves of *Edwardsiphyton* are distinct from rounded apices of *Akdalophyton* (Snigirevskaya *et al*., 1992), rudimentary leaves of *Musciphyton* (Kozlowski & Greguss, 1959), and wide leaves of *Dollyphyton* (Figs 4F, 11A–D, M), *Protosphagnum* and *Vorcutannularia* (Neuburg, 1960). *Muscites* has similar acute linear leaves but an erect capsule with vertical dehiscence (Anderson, 1976).

Edwardsiphyton ovatum new species

Figures 4E, 11N–11U

Holotype—Slab PB2281 (Figs 4E, 11P).

Diagnosis—Axis with helically arranged, narrow acuminate, entire–margined, leaves, 3.8 ± 0.5 mm long, 1.5 ± 0.2 mm wide (n=6), arched outwards from the axis; capsule ovate, 5.1 ± 0.4 mm long, 3.0 ± 0.4 mm wide (n=7), reflexed, on seta 5.4 ± 1.7 mm long and 0.9 ± 0.2 mm wide (n=7); peristome 2.3 ± 0.4 mm diameter (n=7), with 16 attenuate teeth, 2.3 ± 0.4 mm long (n=7) and 0.26 ± 0.03 mm wide at base (n=29), undivided transversely and longitudinally: spores 9 ± 2 µm long (n=19), ellipsoidal, and strongly ornamented with bacculae.

Etymology—The epithet *ovatum* is Latin for egg–shaped in reference to the capsule.

Materials—Slabs PB2254, PB2275, PB2281, and USNM125100. Offcuts from PB 2254 were macerated for slide UOF123854, SEM stubs UOF123863–4, and UOF123867–8, and transfer UOF124276.

Description—Narrow, acutely pointed and outward arching leaves and a reflexed capsule on a long seta distinguish *Edwardsiphyton* from other plants in the Douglas Dam Lagerstätte. The leaves are thick and carbonaceous (Fig. 11N, black in backscatter electron microscopy of Fig. 11Q), and presumably multistratose, but were easily destroyed by acid maceration in Schultz solution. Leaf margins appear entire.

All 7 capsules known are ovate in shape and completely reflexed back toward the shoot apex on a long seta. The body of the capsules is lumpy and irregular, but the reflexed apex shows tapering long teeth on a weakly differentiated peristome (Figs 4E, 11P, R). Only 8 teeth were seen in lateral view of transfers and compressions, and from the way they taper apically, a single circlet of 16 teeth is inferred. Spores found in capsules of *Edwardsiphyton* are small (10 µm diameter: Fig. 7I) and have a strong ornament of verrucae and baculae (Fig. 11S–U).

Remarks— Among dispersed Ordovician spores, those of *Edwardsiphyton* are most like *Rugosphaera* sp. A (Wellman *et al.*, 2015).

Kingdom—Fungi Moore, 1980

Phylum—Glomeromycota Walker & Schüßler, 2004

Class—Glomerales Morton & Benny, 1990

Family—Glomeraceae Morton & Benny, 1990

Genus—*Palaeoglomus* Redecker *et al*., 2002

Type species—*Palaeoglomus grayi* Redecker *et al*., 2002

Palaeoglomus strotheri new species.

Fig. 12

Holotype—SEM stub UOF123864 (Fig. 12A–B).

Diagnosis—Branching aseptate hyphae 5.8 ± 1.8 µm diameter (n=18), with irregular radial arbuscles; vesicles subrectangular 30 ± 7 µm diameter (n=31) with irregular lobes and patches with dense echinate ornament, and other areas finely rugulate; spores ellipsoidal, smooth, with maximum diameter 20 ± 3 µm (n=7)

Description—Aseptate, long hyphae attached to swollen vesicles are common in macerations (Fig. 12D, H–K). The vesicles are elongate and polygonal to spherical, but irregularly shaped and lumpy. They have sparse and clustered spinose ornament, but also lobes that are densely echinate (Fig. 12A–B). They are terminal and lateral on hyphal strands (Fig. 12C, 12H, J–K, M–O). The vesicles can be distinguished from spherical to ovoid smooth unattached spores of comparable size, often with brittle cracks (Fig. 12Q–R). Size range of vesicles is more variable (15–46 µm) than for spores (16–26 µm: Fig. 7G–H). This and morphological variation from smooth to patchily echinate may be an indication that more than one taxon is present in this assemblage.

Most macerated vesicles of *Palaeoglomus strotheri* are free of plant host remnants (Fig. 12A–C, E, J–K, M–P), but some hyphae have basal divergent branches like an arbuscle base (Fig. 12J, M), and transfers show arbuscle–like branching structures (Fig. 12F–G). Arbuscles are evidence that they were

endomycorrhizae, but preservation of invaded tissues (best in Fig. 12L), is inadequate to determine the host species.

Etymology—The specific epithet is in honour of Paul Strother.

Materials—Offcuts of PB2254 were macerated for slide OUF123854, SEM stubs UOF123863–8, and transfer UOF124277.

Remarks—Discovery of this new species of *Palaeoglomus* confirms the Ordovician antiquity of Glomeracean fungi. The Douglas Dam specimens with dark burial alteration compatible with 2.7–5.5 km burial depth (Epstein *et al.*, 1977) from a 20 m excavation (Laurence, 1944) dispel suspicions that *P. strotheri* is contaminating modern fungi, as is plausible for vesicles and spores of *Palaeoglomus grayi* (Redecker *et al*., 2000, 2002) a taxon based on spores, vesicles and hyphae from Middle Ordovician surface exposures of limestones in Wisconsin.

Palaeoglomus grayi has sparsely spinose ornament on vesicles and more globular spores (Redecker *et al*., 2000, 2002), which distinguish it as a separate species. *Palaeoglomus boullardi*, a Devonian species permineralized in the Rhynie Chert (Strullu–Derrien *et al*., 2014), is also more sparsely ornamented, but much larger than *P. strotheri*. *Palaeoglomus grayi* is found isolated from plants within marine limestones, and the host tissue of *P. strotheri* is imperfectly preserved, but *P. boullardi* is found with arbuscles, vesicles and spores within tissues of early land plants as an endomycorrhiza (Strullu Derrien *et al*., 2014). This endomycorrhizal habit is also likely for *Palaeoglomus strotheri* with tissue remnants and associated arbuscles (Fig. 12F–G, J, M). Hornworts are currently symbiotic with endomycorrizhal fungi (Glomeromycota and Mucoromycotina: Carafa *et al*., 2003; Ligrone *et al*., 2007; Wang *et al*., 2010; Bonfante & Selosse, 2010; Desirò *et al*., 2013). Ordovician *Palaeoglomus strotheri* and *P. grayi* may both have been endomycorrhizal like their living relatives, during an early phase of mycotrophic coevolution with land plants (Retallack & Landing, 2014; Retallack, 2015c).

Class—Nematophytales Lang, 1937

Family—Prototaxitaceae Hueber, 2001

Genus—*Prototaxites* Dawson, 1859

Type species—*Prototaxites loganii* Dawson, 1859

Prototaxites honeggeri new species

Figs 4C–D, 13

1956 Caster & Brooks, "spoor" Pl. 23, fig. 6.

Holotype—Slab USNM125084 (Fig. 4C, 13B).

Diagnosis—Erect tapering trunk 13 ± 1 mm diameter (n=5), at least 126 mm long (n=1), with dichotomous terminal branches and 4 additional branches in upper third of trunk; lower portion of trunk hollow and crushed in compression: apical branches 9.4 ± 1.3 mm wide (n=7), transversely wrinkled with squamules 2.6 ± 0.4 mm wide (n=31); skeletal hyphae straight to slightly curved, sparsely branched, aseptate, 10 ± 2 μm diameter (n=28); generative hyphae sparsely septate, commonly branched, curled, 4 ± 1 μm diameter (n=39); some generative hyphae form cortical nests 40 μm diameter, with interior subspherical, spheroidal cells 8 ± 1 μm diameter (n=5), each embraced and indented by 3–5 haustorial threads.

Description—The largest fossils in the Douglas Dam assemblage are pencil–sized stems (Figs 4C–D, 13A–B). The most complete of these has a flattened and striated base, but transverse wrinkles in the upper portion with preserved cortex and four branch bases (Figs 4D, 13A). The wrinkles have higher relief and become pustulose in the stout ellipsoidal branches, including terminal dichotomous branches. The highly wrinkled branches and apical portion of the trunks have high relief compared with the base of the trunk, which is decorticated and shows an internal hollow of sparse tubular strands (Fig. 13C–D). The internal hollow surrounded by a palisade of skeletal hyphae is filled with diagenetically recrystallized clay (Fig. 13D).

The characteristic histology of large skeletal hyphae and small generative hyphae found in *Prototaxites* was revealed especially in fragments on a slab (Fig. 13J). Cortical nests of tapering and curling generative hyphae (Fig. 13F–G, K) and long skeletal hyphae (Fig. 13E, H) were also seen in strew mounts and a Walton transfer. The skeletal hyphae are sparsely branched, aseptate, and 10 ± 2 μm diameter (Fig. 7E). Generative hyphae were sparsely septate, commonly branched, curled, and 4 ± 1 μm diameter (Fig. 7F). One cortical nest of generative hyphae included small (8 ± 1 μm), spheroidal cells gripped by haustorial threads of generative hyphae, like coccoid photobionts of a lichen (Fig. 13K).

Caster & Brooks (1956) regarded the most complete specimen (Fig. 4D, 13A) as "spoor", by which they meant an invertebrate burrow. That interpretation does not explain a variety of observations: differential width and thickness along the length of the fossil, and near orthogonal angles of branching clustered near the tapered apex. In contrast, burrows maintain the same diameter throughout by peristaltic movement of a single trace maker that cannot turn so tightly (Seilacher, 2007).

Etymology—The species name is in honour of Rosmarie Honegger, who has done pioneering work on Devonian lichens.

Materials—Slabs USNM125083, USNM125084, PB2275, and PB2277. Offcuts of PB2254 were macerated to make slide OUF123854, and PB2277 was macerated to make SEM stub UOF123868 and transfer UOF124279.

Remarks—*Prototaxites honeggeri* differs principally from the generotype species *P. loganii* in its much smaller size: 13 mm rather than 360 mm diameter (Retallack & Landing, 2014). An allometric equation for height of nematophytes (Retallack & Landing, 2014) gives 0.45 ± 0.9 m for *P. honeggeri*, a little more than twice the preserved length (Figs 4.4, 13.1), but 8.77 ± 0.9 m for *P. loganii* (Fig. 8H). Small size and lack of growth rings also differentiates *P. honeggeri* from *P. saharianum* (Arbey & Koeniguer, 1979; Guerrak, 1988), *P. lafontii* (Arbey & Koeniguer, 1979), *P. taiti* (Honegger *et al*., 2018), *P. ortoni* (Cross *et al*., 1996) and *P. southwelli* (Arnold, 1952; Boyce *et al*., 2007). There is no indication of growth rings like those of *P. loganii* in *P. honeggeri*, but the branching pattern, hyphal tissues, cortical nests, and presumed green algal symbiont are all very similar. *Prototaxites honeggeri* may have been hollow near the base where there is a ring of vertical skeletal hyphae (Figs 13C–D), unlike other species of *Prototaxites*. The club–shaped short branches of *P. honeggeri* are similar in form, if not size, to those of *P. loganii* (Fig. 8H), and distinct from other nematophytes such as *Germanophyton* with laminar ends to the branches (Høeg, 1942; Retallack, 2015c), and *Mosellophyton* with copious fine branches (Schweitzer, 1983; Retallack, 2015c). *Nematasketum* is different again in having distinct annular thickenings within skeletal hyphae (Edwards & Axe, 2012).

The botanical nature of *Prototaxites* has been controversial, but interpretation as a vascular plant, alga or rolled mat of liverworts has been ruled out by its histology (Retallack & Landing, 2014; Honegger *et al*., 2018). Its fungal affinities have been established securely by pore and wall ultrastructure (Schmid, 1976), but it remains uncertain whether it belongs in Basidiomycota (Hueber, 2001), Ascomycota (Honegger *et al*., 2018), or Glomeromycota–Mucoromycotina (Retallack & Landing, 2014). The skeletal hyphae are aseptate like Glomeromycota, but the generative and binding hyphae are sparsely septate like Mucoromycotina, Basidiomycota and Ascomycota. Fine branching structures in Devonian *Prototaxites loganii* (Hueber, 2001) may be Hartig nets of Basidiomycota or haustoria of Ascomycota, and thus parasitic forms (Retallack & Landing, 2014). A detached hymenium associated with *Prototaxites taitii* has been taken as evidence of ascomycotan affinities (Honegger *et al*., 2018), but may be an accidental association or a parasitic form. It is also possible that single species of *Prototaxites* included hyphae of Basidiomycota, Ascomycota, and Glomeromycota, like modern multispecies lichens (Hawksworth, 1988). One reason to doubt that *Prototaxites honeggeri* is a record of Basidiomycota and Ascomycota, is the current lack of independent evidence from spores or mesofossils of those dikaryan clades before the Devonian (Retallack, 2015a).

The nature of the photobiont is uncertain, although the size (8 μm) and shape of these spheroidal cells (Fig. 13K) is like that of green algal photosymbionts known from Devonian *Prototaxites loganii* (Retallack & Landing, 2014). Even though free–living cyanobacteria are smaller (10 μm) than free–living green algae (25 μm), cyanobacteria become larger as symbionts, but algae in haustorial symbiosis become smaller than 10 μm (Amadjian, 1967; Henley *et al*., 2004).

Prototaxites is mainly known from Silurian and younger rocks (Hueber, 2001; Honegger *et al*., 2018), but a variety of unusually large plant–like fossils may have been Ordovician nematophytes, for example, sandstone casts described as *Lepidotruncus fortis* (Fritsch, 1908), and root–like structures, *Radix corrugatus* (Fritsch, 1908) from the Katian–Hirnantian (Kříž & Pojeta, 1974), Kosov Formation, near Chodouň and Vonoklas (respectively), Czech Republic. Also comparable is *Protostigmaria sigillarioides* (Lesquereux, 1877) from the Late Ordovician (Katian), Waynesville Formation near Lebanon, Ohio (Lesquereux, 1874). Comparable remains (*Lepidotruncus* sp. indet.) are known from Hirnantian, glacial deposits of the El Golea Member, Tamadjert Formation, near Zmeïlet Barka, Algeria (Arbey & Koeniguer, 1979; LeHeron & Craig, 2008), and from the Hirnantian, Juniata Formation at Beans Gap, Tennessee (Retallack, 2015a). Other remains comparable with *Radix* (Fritsch, 1908) are known from the early Katian, Gull River Formation near Ingham Mills, New York (Argast, 1992). The New York root–like fossils are partly permineralized in calcite and show a distinctive histology of tubular cell walls with a carbon isotopic composition (δ^{13}C organic vs. PDB–23.5 to–25 ‰) of land plants, rather than Ordovician marine organic matter (Tomescu *et al*., 2009).

DOUGLAS DAM PALEOCOMMUNITY

The Douglas Dam Lagerstätte includes both arthropods and a variety of fossil plants (Table 1), dominated by hornworts (Fig. 14). The holotype slab of the hornwort *Casterlorum crispum* has 9 individuals equally spaced but separated from each other (Fig. 5A), unlike clonal growth, but similar to early successional communities germinating from spores. Most plants were ground hugging thalli, but *Prototaxites honeggeri* had large tapering stems that would have towered over the others. Glomalean fungi (*Palaeoglomus strotheri*) and permanent tetrads of balloonworts (*Tetrahedraletes grayae*) are more conspicuous in the microfossil assemblage than in the megafossil assemblage, so both taxa were prolific spore and vesicle producers (Fig. 14).

The plants from Douglas Dam can be visualised by comparison with modern plants (Fig. 8), as well as by interpretive sketches (Fig. 4) and artistic restoration (Fig. 15). The setting is a lake margin in the base of a 64–m–deep sinkhole in Mascot Dolomite (Fig. 1). Amphibious *Chasmataspis* may have left footprints (*Diplichnites*) in the mud, but *Douglasiocaris* was likely restricted to the water. The tallest plants are pencil–sized trunks of *Prototaxites*, interpreted here as a lichen with green algal photobiont and Glomeromycotan–Mucoromycotinan hyphae. Glomalean fungi *Palaeoglomus*, also form an endomycorrhizal network

Table 1—Raw measurements of Ordovician land plants (all μm)

Taxon	measure	specimen	microns
Casterlorum crispum	thallus width	USNM125102	3755
Casterlorum crispum	thallus width	USNM125102	4510
Casterlorum crispum	thallus width	USNM125102	2214
Casterlorum crispum	thallus width	USNM125102	2694
Casterlorum crispum	thallus width	USNM125102	3949
Casterlorum crispum	thallus width	USNM125102	5133
Casterlorum crispum	thallus width	USNM125102	4735
Casterlorum crispum	thallus width	USNM125102	4367
Casterlorum crispum	thallus width	USNM125102	5010
Casterlorum crispum	thallus width	USNM125102	5296
Casterlorum crispum	thallus width	USNM125165	5711
Casterlorum crispum	thallus width	USNM125165	5005
Casterlorum crispum	thallus width	USNM125165	5353
Casterlorum crispum	thallus width	USNM125165	5433
Casterlorum crispum	thallus width	USNM645552	4302
Casterlorum crispum	thallus width	USNM645552	3510
Casterlorum crispum	thallus width	USNM645557	3953
Casterlorum crispum	thallus width	USNM645557	3393
Casterlorum crispum	thallus width	USNM645558	7538
Casterlorum crispum	thallus width	PB2251	8886
Casterlorum crispum	thallus width	PB2251	7882
Casterlorum crispum	horn length	USNM125102	25663
Casterlorum crispum	horn length	USNM125102	17459
Casterlorum crispum	horn length	USNM125102	22510
Casterlorum crispum	horn length	USNM128091	64853
Casterlorum crispum	horn length	USNM645551	42381
Casterlorum crispum	horn length	USNM645553	48093
Casterlorum crispum	horn length	USNM645554	45262
Casterlorum crispum	horn length	USNM645555	37802
Casterlorum crispum	horn length	USNM645556	38374
Casterlorum crispum	horn length	USNM645559	58947
Casterlorum crispum	horn length	PB2251	61398
Casterlorum crispum	horn length	USNM128088	77014
Casterlorum crispum	horn length	USNM128089	41786
Casterlorum crispum	horn length	USNM128090	32887
Casterlorum crispum	horn length	USNM128092	41078
Casterlorum crispum	horn width	USNM125102	1092
Casterlorum crispum	horn width	USNM125102	1163
Casterlorum crispum	horn width	USNM125102	990
Casterlorum crispum	horn width	USNM128091	669
Casterlorum crispum	horn width	USNM645551	1181
Casterlorum crispum	horn width	USNM645553	697
Casterlorum crispum	horn width	USNM645554	863
Casterlorum crispum	horn width	USNM645555	737
Casterlorum crispum	horn width	USNM645556	635
Casterlorum crispum	horn width	USNM645559	1137
Casterlorum crispum	horn width	PB2251	1169
Casterlorum crispum	horn width	USNM128088	699
Casterlorum crispum	horn width	USNM128089	759
Casterlorum crispum	horn width	USNM128090	658
Casterlorum crispum	horn width	USNM128092	1258
Casterlorum crispum	involucre length	USNM125102	4469
Casterlorum crispum	involucre length	USNM125102	4816
Casterlorum crispum	involucre length	USNM125102	4388
Casterlorum crispum	involucre length	USNM125102	3755
Casterlorum crispum	involucre length	USNM125102	3429
Casterlorum crispum	involucre length	USNM125102	3959
Casterlorum crispum	involucre length	USNM125102	3449
Casterlorum crispum	involucre length	USNM125102	4143
Casterlorum crispum	involucre length	USNM125102	4367
Casterlorum crispum	involucre length	USNM125102	4337
Casterlorum crispum	involucre length	USNM125102	4122
Casterlorum crispum	involucre length	USNM125102	4949
Casterlorum crispum	involucre length	USNM125165	6507
Casterlorum crispum	involucre length	USNM125165	5861
Casterlorum crispum	involucre length	USNM125165	6458
Casterlorum crispum	involucre length	USNM128091	7018
Casterlorum crispum	involucre length	USNM645551	13313
Casterlorum crispum	involucre length	USNM645552	7143
Casterlorum crispum	involucre length	USNM645555	5107
Casterlorum crispum	involucre length	USNM645556	13291
Casterlorum crispum	involucre length	USNM645558	6907
Casterlorum crispum	involucre length	USNM645558	5280
Casterlorum crispum	involucre length	USNM645559	8305
Casterlorum crispum	involucre length	PB2251	8011
Casterlorum crispum	involucre length	USNM128088	12156
Casterlorum crispum	involucre length	USNM128089	8258
Casterlorum crispum	involucre length	USNM128092	9487
Casterlorum crispum	involucre width	USNM125102	1316
Casterlorum crispum	involucre width	USNM125102	1337
Casterlorum crispum	involucre width	USNM125102	1704
Casterlorum crispum	involucre width	USNM125102	1398
Casterlorum crispum	involucre width	USNM125102	1643
Casterlorum crispum	involucre width	USNM125102	1878
Casterlorum crispum	involucre width	USNM125102	1796
Casterlorum crispum	involucre width	USNM125102	1214
Casterlorum crispum	involucre width	USNM125102	1500
Casterlorum crispum	involucre width	USNM125102	2061
Casterlorum crispum	involucre width	USNM125102	1918
Casterlorum crispum	involucre width	USNM125102	1694
Casterlorum crispum	involucre width	USNM125165	1214
Casterlorum crispum	involucre width	USNM125165	1532
Casterlorum crispum	involucre width	USNM125165	1542
Casterlorum crispum	involucre width	USNM128091	918
Casterlorum crispum	involucre width	USNM645551	1278
Casterlorum crispum	involucre width	USNM645552	1143
Casterlorum crispum	involucre width	USNM645555	2051
Casterlorum crispum	involucre width	USNM645556	1410
Casterlorum crispum	involucre width	USNM645558	1556
Casterlorum crispum	involucre width	USNM645558	916
Casterlorum crispum	involucre width	USNM645559	1842
Casterlorum crispum	involucre width	PB2251	1723
Casterlorum crispum	involucre width	USNM128088	1564
Casterlorum crispum	involucre width	USNM128089	1111
Casterlorum crispum	involucre width	USNM128092	1322
Casterlorum crispum	rhizoid width	USNM125102	357
Casterlorum crispum	rhizoid width	USNM125102	551
Casterlorum crispum	rhizoid width	USNM125102	561
Casterlorum crispum	rhizoid width	USNM125102	561

Casterlorum crispum	rhizoid length	USNM125102	2388
Casterlorum crispum	rhizoid length	USNM125102	2806
Casterlorum crispum	rhizoid length	USNM125102	4061
Casterlorum crispum	rhizoid length	USNM125102	5520
Casterlorum crispum	rhizoid length	USNM125102	6071
Casterlorum crispum	rhizoid length	USNM125102	6633
Casterlorum crispum	spore width	UOF123854	6
Casterlorum crispum	spore width	UOF123854	9
Casterlorum crispum	spore width	UOF123854	6
Casterlorum crispum	spore width	UOF123854	5
Casterlorum crispum	spore width	UOF123854	6
Casterlorum crispum	spore width	UOF123854	8
Casterlorum crispum	spore width	UOF123854	8
Casterlorum crispum	spore width	UOF123854	8
Casterlorum crispum	spore width	UOF123854	10
Casterlorum crispum	spore width	UOF123854	10
Casterlorum crispum	spore width	UOF123854	10
Casterlorum crispum	spore width	UOF123854	9
Casterlorum crispum	spore width	UOF123854	6
Casterlorum crispum	spore width	UOF123854	11
Casterlorum crispum	spore width	UOF123854	11
Casterlorum crispum	spore width	UOF123854	8
Casterlorum crispum	spore width	UOF123854	9
Casterlorum crispum	spore width	UOF123854	9
Casterlorum crispum	spore width	UOF123854	7
Casterlorum crispum	spore width	UOF123854	8
Casterlorum crispum	spore width	UOF123854	9
Casterlorum crispum	spore width	UOF123854	8
Casterlorum crispum	spore width	UOF123854	9
Casterlorum crispum	spore width	UOF123864	12
Casterlorum crispum	spore width	UOF123865	15
Casterlorum crispum	spore width	UOF123865	11
Casterlorum crispum	spore width	UOF123865	12
Casterlorum crispum	spore length	UOF123854	13
Casterlorum crispum	spore length	UOF123854	11
Casterlorum crispum	spore length	UOF123854	9
Casterlorum crispum	spore length	UOF123854	8
Casterlorum crispum	spore length	UOF123854	12
Casterlorum crispum	spore length	UOF123854	10
Casterlorum crispum	spore length	UOF123854	12
Casterlorum crispum	spore length	UOF123854	12
Casterlorum crispum	spore length	UOF123854	11
Casterlorum crispum	spore length	UOF123854	13
Casterlorum crispum	spore length	UOF123854	11
Casterlorum crispum	spore length	UOF123854	13
Casterlorum crispum	spore length	UOF123854	9
Casterlorum crispum	spore length	UOF123854	16
Casterlorum crispum	spore length	UOF123854	16
Casterlorum crispum	spore length	UOF123854	10
Casterlorum crispum	spore length	UOF123854	11
Casterlorum crispum	spore length	UOF123854	12
Casterlorum crispum	spore length	UOF123854	13
Casterlorum crispum	spore length	UOF123854	12
Casterlorum crispum	spore length	UOF123854	13
Casterlorum crispum	spore length	UOF123854	10
Casterlorum crispum	spore length	UOF123854	10
Casterlorum crispum	spore length	UOF123864	18
Casterlorum crispum	spore length	UOF123865	17
Casterlorum crispum	spore length	UOF123865	16
Casterlorum crispum	spore length	UOF123865	15
Casterlorum crispum	columella diameter	UOF123854	6
Casterlorum crispum	columella diameter	UOF123854	10
Casterlorum crispum	columella diameter	UOF123854	8
Casterlorum crispum	columella diameter	UOF123854	9
Casterlorum crispum	columella diameter	UOF123854	5
Casterlorum crispum	columella diameter	UOF123863	4
Casterlorum crispum	pseudoelater length	UOF123854	20
Casterlorum crispum	pseudoelater length	UOF123854	24
Casterlorum crispum	pseudoelater length	UOF123854	21
Casterlorum crispum	pseudoelater length	UOF123854	16
Casterlorum crispum	pseudoelater length	UOF123854	15
Casterlorum crispum	pseudoelater length	UOF123864	17
Casterlorum crispum	pseudoelater length	UOF123865	12
Casterlorum crispum	pseudoelater length	UOF123865	10
Casterlorum crispum	pseudoelater width	UOF123854	8
Casterlorum crispum	pseudoelater width	UOF123854	8
Casterlorum crispum	pseudoelater width	UOF123854	6
Casterlorum crispum	pseudoelater width	UOF123854	8
Casterlorum crispum	pseudoelater width	UOF123854	5
Casterlorum crispum	pseudoelater width	UOF123864	5
Casterlorum crispum	pseudoelater width	UOF123865	4
Casterlorum crispum	pseudoelater width	UOF123865	4
Casterlorum crispum	Cyano. fil. width	UOF123868	3
Casterlorum crispum	Nostoc fil. width	UOF123868	4
Casterlorum crispum	Nostoc fil. width	UOF123868	4
Casterlorum crispum	Nostoc fil. width	UOF123868	4
Casterlorum crispum	Nostoc fil. length	UOF123868	11
Casterlorum crispum	Nostoc fil. length	UOF123868	13
Casterlorum crispum	Nostoc fil. length	UOF123868	12
Casterlorum crispum	Nostoc fil. length	UOF123868	9
Casterlorum crispum	Nostoc cell length	UOF123868	3
Casterlorum crispum	Nostoc cell length	UOF123868	3
Casterlorum crispum	Nostoc cell length	UOF123868	3
Casterlorum crispum	Nostoc cell length	UOF123868	2
Casterlorum crispum	Nostoc cell length	UOF123868	3
Casterlorum crispum	Nostoc cell length	UOF123868	3
Casterlorum crispum	Nostoc cell length	UOF123868	3
Casterlorum crispum	Nostoc cell length	UOF123868	3
Casterlorum crispum	Nostoc cell length	UOF123868	3
Casterlorum crispum	Nostoc cell length	UOF123868	3
Casterlorum crispum	Nostoc cell length	UOF123868	4
Cestites mirabilis	thallus width	USNM125087	3351
Cestites mirabilis	thallus width	USNM125087	2967
Cestites mirabilis	thallus width	USNM125087	2604
Cestites mirabilis	thallus width	USNM645561	3820
Cestites mirabilis	thallus width	USNM645561	2870
Cestites mirabilis	thallus width	USNM645561	3056
Cestites mirabilis	thallus width	USNM645562	1903
Cestites mirabilis	thallus width	USNM645562	1544
Cestites mirabilis	thallus width	USNM645560	2739
Cestites mirabilis	thallus width	PB2266A	2398
Cestites mirabilis	thallus width	USNM125106	4908
Cestites mirabilis	thallus width	USNM125106	4512
Cestites mirabilis	thallus width	USNM125106	4462

Cestites mirabilis	midrib width	USNM125087	1889
Cestites mirabilis	midrib width	USNM125087	1825
Cestites mirabilis	midrib width	USNM125087	1409
Cestites mirabilis	midrib width	USNM645561	1105
Cestites mirabilis	midrib width	USNM645561	1621
Cestites mirabilis	midrib width	USNM645561	1383
Cestites mirabilis	midrib width	USNM645562	757
Cestites mirabilis	midrib width	USNM645562	546
Cestites mirabilis	midrib width	USNM645560	2000
Cestites mirabilis	midrib width	PB2266A	1052
Cestites mirabilis	midrib width	USNM125106	2281
Cestites mirabilis	midrib width	USNM125106	2201
Cestites mirabilis	midrib width	USNM125106	2459
Cestites mirabilis	arch. diameter	PB266A	3530
Cestites mirabilis	arch. diameter	PB266A	1860
Cestites mirabilis	arch. diameter	PB266A	3180
Cestites mirabilis	arch. diameter	PB266A	1780
Cestites mirabilis	arch. diameter	PB266A	3550
Cestites mirabilis	arch. diameter	PB266A	4340
Cestites mirabilis	arch. diameter	PB266A	4890
Cestites mirabilis	arch. diameter	PB266A	5240
Cestites mirabilis	arch. diameter	PB266A	5520
Cestites mirabilis	arch. diameter	PB266A	5270
Cestites mirabilis	arch. diameter	PB266A	5810
Cestites mirabilis	arch. diameter	PB266A	6660
Cestites mirabilis	arch. diameter	PB266A	4750
Cestites mirabilis	arch. diameter	PB266A	5340
Cestites mirabilis	arch. stalk diameter	PB266A	970
Cestites mirabilis	arch. stalk diameter	PB266A	940
Cestites mirabilis	arch. stalk diameter	PB266A	670
Cestites mirabilis	arch. stalk diameter	PB266A	540
Cestites mirabilis	arch. stalk diameter	PB266A	870
Cestites mirabilis	arch. stalk diameter	PB266A	1010
Cestites mirabilis	arch. stalk diameter	PB266A	1080
Cestites mirabilis	arch. stalk diameter	PB266A	840
Cestites mirabilis	arch. stalk length	PB266A	7730
Cestites mirabilis	arch. stalk length	PB266A	8920
Cestites mirabilis	arch. stalk length	PB266A	13730
Cestites mirabilis	arch. stalk length	PB266A	5770
Cestites mirabilis	arch. stalk length	PB266A	7790
Cestites mirabilis	arch. stalk length	PB266A	7890
Cestites mirabilis	arch. stalk length	PB266A	7990
Cestites mirabilis	spore diameter	UOF123867	47
Cestites mirabilis	spore diameter	UOF123867	36
Cestites mirabilis	spore diameter	UOF123868	26
Cestites mirabilis	spore diameter	UOF123867	49
Cestites mirabilis	spore diameter	PB2269	49
Cestites mirabilis	spore diameter	PB2269	45
Cestites mirabilis	spore diameter	PB2269	44
Cestites mirabilis	spore diameter	PB2269	43
Cestites mirabilis	spore diameter	PB2269	47
Cestites mirabilis	spore diameter	PB2269	48
Cestites mirabilis	spore diameter	PB2269	48
Cestites mirabilis	spore diameter	PB2269	46
Cestites mirabilis	spore diameter	PB2269	46
Cestites mirabilis	spore diameter	PB2269	47
Cestites mirabilis	spore diameter	PB2269	47
Cestites mirabilis	spore diameter	PB2269	47
Cestites mirabilis	rhizoid diameter	UOF123868	20
Cestites mirabilis	rhizoid diameter	UOF123868	30
Cestites mirabilis	rhizoid diameter	UOF123868	14
Cestites mirabilis	rhizoid diameter	UOF123868	21
Cestites mirabilis	rhizoid diameter	UOF123868	18
Cestites mirabilis	rhizoid diameter	UOF123868	20
Cestites mirabilis	rhizoid diameter	UOF123868	16
Cestites mirabilis	ventral scale length	UOF123868	68
Cestites mirabilis	ventral scale length	UOF123868	28
Cestites mirabilis	ventral scale length	UOF123868	56
Cestites mirabilis	ventral scale length	UOF123868	67
Cestites mirabilis	ventral scale length	UOF123868	54
Cestites mirabilis	ventral scale width	UOF123868	36
Cestites mirabilis	ventral scale width	UOF123868	16
Cestites mirabilis	ventral scale width	UOF123868	34
Cestites mirabilis	ventral scale width	UOF123868	37
Cestites mirabilis	ventral scale width	UOF123868	31
Janegraya sibylla	pseudoper. diameter	PB2254	355
Janegraya sibylla	pseudoper. diameter	PB2254	457
Janegraya sibylla	pseudoper. diameter	PB2254	442
Janegraya sibylla	pseudoper. diameter	PB2254	426
Janegraya sibylla	pseudoper. diameter	PB2254	397
Janegraya sibylla	pseudoper. diameter	PB2254	441
Janegraya sibylla	pseudoper. diameter	PB2254	482
Janegraya sibylla	pseudoper. diameter	PB2254	348
Janegraya sibylla	pseudoper. diameter	PB2254	355
Janegraya sibylla	pseudoper. diameter	PB2254	363
Janegraya sibylla	pseudoper. diameter	PB2254	362
Janegraya sibylla	pseudoper. diameter	PB2254	337
Janegraya sibylla	pseudoper. diameter	PB2254	332
Janegraya sibylla	pseudoper. diameter	PB2254	387
Janegraya sibylla	pseudoper. diameter	PB2254	355
Janegraya sibylla	pseudoper. diameter	PB2254	302
Janegraya sibylla	pseudoper. diameter	PB2254	315
Janegraya sibylla	pseudoper. length	PB2254	478
Janegraya sibylla	pseudoper. length	PB2254	489
Janegraya sibylla	pseudoper. length	PB2254	393
Janegraya sibylla	pseudoper. length	PB2254	469
Janegraya sibylla	pseudoper. length	PB2254	430
Janegraya sibylla	pseudoper. length	PB2254	460
Janegraya sibylla	pseudoper. length	PB2254	414
Janegraya sibylla	pseudoper. length	PB2254	441
Janegraya sibylla	pseudoper. length	PB2254	424
Janegraya sibylla	pseudoper. length	PB2254	426
Janegraya sibylla	pseudoper. length	PB2254	347
Janegraya sibylla	sporangium diameter	PB2254	99
Janegraya sibylla	sporangium diameter	PB2254	99
Janegraya sibylla	sporangium diameter	PB2254	91
Janegraya sibylla	sporangium diameter	PB2254	90
Janegraya sibylla	sporangium diameter	PB2254	89
Janegraya sibylla	sporangium diameter	PB2254	97
Janegraya sibylla	sporangium diameter	PB2254	98
Janegraya sibylla	sporangium diameter	PB2254	128
Janegraya sibylla	sporangium diameter	PB2254	73
Janegraya sibylla	sporangium diameter	PB2254	76
Janegraya sibylla	sporangium diameter	PB2254	80

Janegraya sibylla	sporangium diameter	PB2254	100
Janegraya sibylla	sporangium diameter	PB2254	110
Janegraya sibylla	sporangium diameter	PB2254	125
Janegraya sibylla	sporangium diameter	PB2254	126
Janegraya sibylla	sporangium diameter	PB2254	109
Janegraya sibylla	sporangium diameter	PB2254	133
Janegraya sibylla	sporangium diameter	PB2254	104
Janegraya sibylla	sporangium diameter	PB2254	105
Janegraya sibylla	sporangium diameter	PB2254	104
Janegraya sibylla	sporangium diameter	PB2254	106
Janegraya sibylla	sporangium diameter	PB2254	119
Janegraya sibylla	sporangium diameter	PB2254	114
Janegraya sibylla	tetrad diameter	UOF123854	14
Janegraya sibylla	tetrad diameter	UOF123854	16
Janegraya sibylla	tetrad diameter	UOF123854	15
Janegraya sibylla	tetrad diameter	UOF123854	12
Janegraya sibylla	tetrad diameter	UOF123854	14
Janegraya sibylla	tetrad diameter	UOF123854	18
Janegraya sibylla	tetrad diameter	UOF123854	18
Janegraya sibylla	tetrad diameter	UOF123854	24
Janegraya sibylla	tetrad diameter	UOF123854	15
Janegraya sibylla	tetrad diameter	UOF123854	22
Janegraya sibylla	tetrad diameter	UOF123854	21
Janegraya sibylla	tetrad diameter	UOF123854	23
Janegraya sibylla	tetrad diameter	UOF123854	20
Janegraya sibylla	tetrad diameter	UOF123854	17
Janegraya sibylla	tetrad diameter	UOF123854	18
Janegraya sibylla	tetrad diameter	UOF123854	20
Janegraya sibylla	tetrad diameter	PB2254	10
Janegraya sibylla	tetrad diameter	UOF123863	21
Janegraya sibylla	tetrad diameter	UOF123863	8
Janegraya sibylla	tetrad diameter	UOF123864	17
Janegraya sibylla	tetrad diameter	UOF123867	12
Janegraya sibylla	spore diameter	UOF123854	6
Janegraya sibylla	spore diameter	UOF123854	6
Janegraya sibylla	spore diameter	UOF123854	8
Janegraya sibylla	spore diameter	UOF123854	8
Janegraya sibylla	spore diameter	UOF123854	10
Janegraya sibylla	spore diameter	UOF123854	9
Janegraya sibylla	spore diameter	UOF123854	9
Janegraya sibylla	spore diameter	UOF123854	10
Janegraya sibylla	spore diameter	UOF123854	11
Janegraya sibylla	spore diameter	UOF123854	12
Janegraya sibylla	spore diameter	UOF123854	8
Janegraya sibylla	spore diameter	UOF123854	10
Janegraya sibylla	spore diameter	UOF123854	7
Janegraya sibylla	spore diameter	UOF123854	11
Janegraya sibylla	spore diameter	UOF123854	8
Janegraya sibylla	spore diameter	UOF123854	13
Janegraya sibylla	spore diameter	UOF123854	12
Janegraya sibylla	spore diameter	UOF123854	14
Janegraya sibylla	spore diameter	UOF123854	12
Janegraya sibylla	spore diameter	UOF123854	10
Janegraya sibylla	spore diameter	UOF123854	15
Janegraya sibylla	spore diameter	UOF123854	17
Janegraya sibylla	spore diameter	UOF123854	16
Janegraya sibylla	spore diameter	UOF123854	14
Janegraya sibylla	spore diameter	UOF123854	12
Janegraya sibylla	spore diameter	UOF123854	12
Janegraya sibylla	spore diameter	UOF123854	11
Janegraya sibylla	spore diameter	UOF123854	17
Janegraya sibylla	spore diameter	UOF123854	17
Janegraya sibylla	spore diameter	UOF123854	17
Janegraya sibylla	spore diameter	UOF123854	14
Janegraya sibylla	spore diameter	UOF123854	14
Janegraya sibylla	spore diameter	UOF123854	13
Janegraya sibylla	spore diameter	UOF123854	19
Janegraya sibylla	spore diameter	UOF123854	20
Janegraya sibylla	spore diameter	UOF123854	19
Janegraya sibylla	spore diameter	UOF123854	15
Janegraya sibylla	spore diameter	UOF123854	17
Janegraya sibylla	spore diameter	UOF123854	14
Janegraya sibylla	spore diameter	UOF123854	15
Janegraya sibylla	spore diameter	UOF123854	15
Janegraya sibylla	spore diameter	UOF123854	13
Janegraya sibylla	spore diameter	UOF123854	13
Janegraya sibylla	spore diameter	UOF123854	13
Janegraya sibylla	spore diameter	UOF123854	12
Janegraya sibylla	spore diameter	UOF123854	13
Janegraya sibylla	spore diameter	UOF123854	15
Janegraya sibylla	spore diameter	UOF123854	13
Janegraya sibylla	spore diameter	PB2254	7
Janegraya sibylla	spore diameter	PB2254	8
Janegraya sibylla	spore diameter	PB2254	7
Janegraya sibylla	spore diameter	UOF123863	20
Janegraya sibylla	spore diameter	UOF123863	18
Janegraya sibylla	spore diameter	UOF123863	7
Janegraya sibylla	spore diameter	UOF123863	7
Janegraya sibylla	spore diameter	UOF123863	7
Janegraya sibylla	spore diameter	UOF123864	15
Janegraya sibylla	spore diameter	UOF123864	13
Janegraya sibylla	spore diameter	UOF123864	13
Janegraya sibylla	spore diameter	UOF123864	13
Janegraya sibylla	spore diameter	UOF123867	10
Janegraya sibylla	spore diameter	UOF123867	8
Janegraya sibylla	spore diameter	UOF123867	8
Dollyphyton boucotii	leaf width	USNM645801	1351
Dollyphyton boucotii	leaf width	USNM645801	1523
Dollyphyton boucotii	leaf width	USNM645801	1639
Dollyphyton boucotii	leaf width	USNM645801	1838
Dollyphyton boucotii	leaf width	USNM645801	1831
Dollyphyton boucotii	leaf width	USNM645801	1907
Dollyphyton boucotii	leaf width	USNM645801	2030
Dollyphyton boucotii	leaf length	USNM645801	4355
Dollyphyton boucotii	leaf length	USNM645801	4170
Dollyphyton boucotii	leaf length	USNM645801	4719
Dollyphyton boucotii	leaf length	USNM645801	4547
Dollyphyton boucotii	leaf length	USNM645801	5110
Dollyphyton boucotii	leaf length	USNM645801	3875
Dollyphyton boucotii	leaf length	USNM645801	4170
Dollyphyton boucotii	capsule length	USNM645801	5237
Dollyphyton boucotii	capsule length	PB2275	3860
Dollyphyton boucotii	capsule width	USNM645801	3311
Dollyphyton boucotii	capsule width	PB2275	2750

Dollyphyton boucotii	pseudopodium length	USNM645801	1186
Dollyphyton boucotii	pseudopodium length	PB2275	2060
Dollyphyton boucotii	Pseudopod. diameter	USNM645801	1452
Dollyphyton boucotii	Pseudopod. diameter	PB2275	1120
Dollyphyton boucotii	operculum diameter	USNM645801	1979
Dollyphyton boucotii	operculum diameter	PB2275	1670
Dollyphyton boucotii	spore length	OUF123854	19
Dollyphyton boucotii	spore length	OUF123854	23
Dollyphyton boucotii	spore length	OUF123854	20
Dollyphyton boucotii	spore length	OUF123854	22
Dollyphyton boucotii	spore length	OUF123854	26
Dollyphyton boucotii	spore length	OUF123854	34
Dollyphyton boucotii	spore length	PB2275	24
Dollyphyton boucotii	spore width	OUF123854	17
Dollyphyton boucotii	spore width	OUF123854	21
Dollyphyton boucotii	spore width	OUF123854	14
Dollyphyton boucotii	spore width	OUF123854	18
Dollyphyton boucotii	spore width	OUF123854	20
Dollyphyton boucotii	spore width	OUF123854	22
Dollyphyton boucotii	spore width	PB2275	12
Edwardsiphyton ovatum	leaf width	USNM125100	1801
Edwardsiphyton ovatum	leaf width	USNM125100	1490
Edwardsiphyton ovatum	leaf width	USNM125100	1463
Edwardsiphyton ovatum	leaf width	USNM125100	1618
Edwardsiphyton ovatum	leaf width	USNM125100	1554
Edwardsiphyton ovatum	leaf width	USNM125100	1252
Edwardsiphyton ovatum	leaf length	USNM125100	3455
Edwardsiphyton ovatum	leaf length	USNM125100	3830
Edwardsiphyton ovatum	leaf length	USNM125100	3912
Edwardsiphyton ovatum	leaf length	USNM125100	3940
Edwardsiphyton ovatum	leaf length	USNM125100	4735
Edwardsiphyton ovatum	leaf length	USNM125100	3172
Edwardsiphyton ovatum	capsule length	USNM125100	4826
Edwardsiphyton ovatum	capsule length	USNM125100	4911
Edwardsiphyton ovatum	capsule length	USNM125100	5690
Edwardsiphyton ovatum	capsule length	UOF124276	5559
Edwardsiphyton ovatum	capsule length	PB2281	4700
Edwardsiphyton ovatum	capsule length	PB2281	4520
Edwardsiphyton ovatum	capsule length	PB2281	5290
Edwardsiphyton ovatum	capsule width	USNM125100	2573
Edwardsiphyton ovatum	capsule width	USNM125100	2601
Edwardsiphyton ovatum	capsule width	USNM125100	3418
Edwardsiphyton ovatum	capsule width	UOF124276	3369
Edwardsiphyton ovatum	capsule width	PB2281	2880
Edwardsiphyton ovatum	capsule width	PB2281	2740
Edwardsiphyton ovatum	capsule width	PB2281	3660
Edwardsiphyton ovatum	seta length	USNM125100	4836
Edwardsiphyton ovatum	seta length	USNM125100	7202
Edwardsiphyton ovatum	seta length	USNM125100	4779
Edwardsiphyton ovatum	seta length	UOF124276	7348
Edwardsiphyton ovatum	seta length	PB2281	2970
Edwardsiphyton ovatum	seta length	PB2281	5180
Edwardsiphyton ovatum	seta length	PB2281	3300
Edwardsiphyton ovatum	seta diameter	USNM125100	864
Edwardsiphyton ovatum	seta diameter	USNM125100	958
Edwardsiphyton ovatum	seta diameter	USNM125100	685
Edwardsiphyton ovatum	seta diameter	UOF124276	858
Edwardsiphyton ovatum	seta diameter	PB2281	1370
Edwardsiphyton ovatum	seta diameter	PB2281	1220
Edwardsiphyton ovatum	seta diameter	PB2281	1140
Edwardsiphyton ovatum	peristome diameter	USNM125100	1934
Edwardsiphyton ovatum	peristome diameter	USNM125100	1953
Edwardsiphyton ovatum	peristome diameter	USNM125100	2469
Edwardsiphyton ovatum	peristome diameter	UOF124276	2929
Edwardsiphyton ovatum	peristome diameter	PB2281	2420
Edwardsiphyton ovatum	peristome diameter	PB2281	2370
Edwardsiphyton ovatum	peristome diameter	PB2281	2230
Edwardsiphyton ovatum	tooth length	USNM125100	1981
Edwardsiphyton ovatum	tooth length	USNM125100	2272
Edwardsiphyton ovatum	tooth length	USNM125100	2385
Edwardsiphyton ovatum	tooth length	UOF124276	2374
Edwardsiphyton ovatum	tooth length	PB2281	2290
Edwardsiphyton ovatum	tooth length	PB2281	1980
Edwardsiphyton ovatum	tooth length	PB2281	2290
Edwardsiphyton ovatum	basal tooth width	USNM125100	235
Edwardsiphyton ovatum	basal tooth width	USNM125100	254
Edwardsiphyton ovatum	basal tooth width	USNM125100	244
Edwardsiphyton ovatum	basal tooth width	USNM125100	263
Edwardsiphyton ovatum	basal tooth width	USNM125100	310
Edwardsiphyton ovatum	basal tooth width	USNM125100	225
Edwardsiphyton ovatum	basal tooth width	USNM125100	272
Edwardsiphyton ovatum	basal tooth width	USNM125100	300
Edwardsiphyton ovatum	basal tooth width	USNM125100	338
Edwardsiphyton ovatum	basal tooth width	USNM125100	272
Edwardsiphyton ovatum	basal tooth width	USNM125100	263
Edwardsiphyton ovatum	basal tooth width	USNM125100	225
Edwardsiphyton ovatum	basal tooth width	UOF124276	260
Edwardsiphyton ovatum	basal tooth width	UOF124276	277
Edwardsiphyton ovatum	basal tooth width	UOF124276	325
Edwardsiphyton ovatum	basal tooth width	UOF124276	270
Edwardsiphyton ovatum	basal tooth width	UOF124276	273
Edwardsiphyton ovatum	basal tooth width	UOF124276	216
Edwardsiphyton ovatum	basal tooth width	UOF124276	238
Edwardsiphyton ovatum	basal tooth width	UOF124276	198
Edwardsiphyton ovatum	basal tooth width	PB2281	300
Edwardsiphyton ovatum	basal tooth width	PB2281	380
Edwardsiphyton ovatum	basal tooth width	PB2281	360
Edwardsiphyton ovatum	basal tooth width	PB2281	330
Edwardsiphyton ovatum	basal tooth width	PB2281	340
Edwardsiphyton ovatum	basal tooth width	PB2281	350
Edwardsiphyton ovatum	basal tooth width	PB2281	360
Edwardsiphyton ovatum	basal tooth width	PB2281	370
Edwardsiphyton ovatum	basal tooth width	PB2281	380
Edwardsiphyton ovatum	spore diameter	OUF123854	10
Edwardsiphyton ovatum	spore diameter	OUF123854	11
Edwardsiphyton ovatum	spore diameter	OUF123854	12
Edwardsiphyton ovatum	spore diameter	OUF123854	9
Edwardsiphyton ovatum	spore diameter	OUF123854	7
Edwardsiphyton ovatum	spore diameter	OUF123854	6
Edwardsiphyton ovatum	spore diameter	OUF123854	9
Edwardsiphyton ovatum	spore diameter	OUF123854	6
Edwardsiphyton ovatum	spore diameter	OUF123854	7
Edwardsiphyton ovatum	spore diameter	OUF123854	11
Edwardsiphyton ovatum	spore diameter	OUF123854	10

Edwardsiphyton ovatum	spore diameter	OUF123854	10
Edwardsiphyton ovatum	spore diameter	OUF123854	12
Edwardsiphyton ovatum	spore diameter	OUF123854	9
Edwardsiphyton ovatum	spore diameter	OUF123854	11
Edwardsiphyton ovatum	spore diameter	OUF123854	11
Edwardsiphyton ovatum	spore diameter	OUF123854	13
Edwardsiphyton ovatum	spore diameter	OUF123854	13
Edwardsiphyton ovatum	spore diameter	OUF123854	9
Palaeoglomus strotheri	hyphal diameter	OUF123854	6
Palaeoglomus strotheri	hyphal diameter	OUF123854	7
Palaeoglomus strotheri	hyphal diameter	OUF123854	4
Palaeoglomus strotheri	hyphal diameter	OUF123854	7
Palaeoglomus strotheri	hyphal diameter	OUF123854	5
Palaeoglomus strotheri	hyphal diameter	OUF123854	5
Palaeoglomus strotheri	hyphal diameter	OUF123854	7
Palaeoglomus strotheri	hyphal diameter	OUF123854	8
Palaeoglomus strotheri	hyphal diameter	OUF123854	7
Palaeoglomus strotheri	hyphal diameter	OUF123854	5
Palaeoglomus strotheri	hyphal diameter	OUF123854	4
Palaeoglomus strotheri	hyphal diameter	OUF123854	3
Palaeoglomus strotheri	hyphal diameter	OUF123854	5
Palaeoglomus strotheri	hyphal diameter	UOF123865	4
Palaeoglomus strotheri	hyphal diameter	UOF123867	11
Palaeoglomus strotheri	hyphal diameter	UOF123868	4
Palaeoglomus strotheri	vesicle diameter	OUF123854	30
Palaeoglomus strotheri	vesicle diameter	OUF123854	24
Palaeoglomus strotheri	vesicle diameter	OUF123854	21
Palaeoglomus strotheri	vesicle diameter	OUF123854	27
Palaeoglomus strotheri	vesicle diameter	OUF123854	26
Palaeoglomus strotheri	vesicle diameter	OUF123854	38
Palaeoglomus strotheri	vesicle diameter	OUF123854	20
Palaeoglomus strotheri	vesicle diameter	OUF123854	33
Palaeoglomus strotheri	vesicle diameter	OUF123854	15
Palaeoglomus strotheri	vesicle diameter	OUF123854	25
Palaeoglomus strotheri	vesicle diameter	OUF123854	31
Palaeoglomus strotheri	vesicle diameter	OUF123854	26
Palaeoglomus strotheri	vesicle diameter	UOF123863	30
Palaeoglomus strotheri	vesicle diameter	UOF123864	31
Palaeoglomus strotheri	vesicle diameter	UOF123864	38
Palaeoglomus strotheri	vesicle diameter	UOF123864	37
Palaeoglomus strotheri	vesicle diameter	UOF123864	37
Palaeoglomus strotheri	vesicle diameter	UOF123864	30
Palaeoglomus strotheri	vesicle diameter	UOF123864	33
Palaeoglomus strotheri	vesicle diameter	UOF123864	31
Palaeoglomus strotheri	vesicle diameter	UOF123864	29
Palaeoglomus strotheri	vesicle diameter	UOF123864	35
Palaeoglomus strotheri	vesicle diameter	UOF123864	27
Palaeoglomus strotheri	vesicle diameter	UOF123864	31
Palaeoglomus strotheri	vesicle diameter	UOF123864	38
Palaeoglomus strotheri	vesicle diameter	UOF123864	35
Palaeoglomus strotheri	vesicle diameter	UOF123864	40
Palaeoglomus strotheri	vesicle diameter	UOF123865	27
Palaeoglomus strotheri	vesicle diameter	UOF123867	46
Palaeoglomus strotheri	vesicle diameter	UOF123868	27
Palaeoglomus strotheri	vesicle diameter	UOF123863	17
Palaeoglomus strotheri	spore diameter	OUF123854	17
Palaeoglomus strotheri	spore diameter	OUF123854	18
Palaeoglomus strotheri	spore diameter	OUF123854	18
Palaeoglomus strotheri	spore diameter	OUF123854	18
Palaeoglomus strotheri	spore diameter	OUF123854	26
Palaeoglomus strotheri	spore diameter	OUF123854	23
Palaeoglomus strotheri	spore diameter	OUF123854	19
Prototaxites honeggeri	stem diameter	USNM125084	11052
Prototaxites honeggeri	stem diameter	USNM125084	11796
Prototaxites honeggeri	stem diameter	USNM125083	13790
Prototaxites honeggeri	stem diameter	USNM125083	13695
Prototaxites honeggeri	stem diameter	USNM125083	13505
Prototaxites honeggeri	stem diameter	USNM125083	13048
Prototaxites honeggeri	stem diameter	USNM125083	13352
Prototaxites honeggeri	branch diameter	USNM125084	9702
Prototaxites honeggeri	branch diameter	USNM125084	7996
Prototaxites honeggeri	branch diameter	USNM125083	12038
Prototaxites honeggeri	branch diameter	USNM125083	9714
Prototaxites honeggeri	branch diameter	USNM125083	7924
Prototaxites honeggeri	branch diameter	USNM125083	9676
Prototaxites honeggeri	branch diameter	USNM125083	8990
Prototaxites honeggeri	squamule width	USNM125084	1736
Prototaxites honeggeri	squamule width	USNM125084	2044
Prototaxites honeggeri	squamule width	USNM125084	2192
Prototaxites honeggeri	squamule width	USNM125084	2748
Prototaxites honeggeri	squamule width	USNM125084	3085
Prototaxites honeggeri	squamule width	USNM125084	3155
Prototaxites honeggeri	squamule width	USNM125084	2798
Prototaxites honeggeri	squamule width	USNM125084	3175
Prototaxites honeggeri	squamule width	USNM125084	2589
Prototaxites honeggeri	squamule width	USNM125084	3125
Prototaxites honeggeri	squamule width	USNM125084	2579
Prototaxites honeggeri	squamule width	USNM125084	3373
Prototaxites honeggeri	squamule width	USNM125084	3552
Prototaxites honeggeri	squamule width	USNM125084	2252
Prototaxites honeggeri	squamule width	USNM125084	2163
Prototaxites honeggeri	squamule width	USNM125084	2351
Prototaxites honeggeri	squamule width	USNM125084	2173
Prototaxites honeggeri	squamule width	USNM125084	1944
Prototaxites honeggeri	squamule width	USNM125084	2341
Prototaxites honeggeri	squamule width	USNM125084	2847
Prototaxites honeggeri	squamule width	USNM125084	2192
Prototaxites honeggeri	squamule width	USNM125084	2847
Prototaxites honeggeri	squamule width	USNM125084	2659
Prototaxites honeggeri	squamule width	USNM125084	2649
Prototaxites honeggeri	squamule width	USNM125084	2302
Prototaxites honeggeri	squamule width	USNM125084	2312
Prototaxites honeggeri	squamule width	USNM125084	2490
Prototaxites honeggeri	squamule width	USNM125084	2242
Prototaxites honeggeri	squamule width	USNM125084	2401
Prototaxites honeggeri	squamule width	USNM125084	2411
Prototaxites honeggeri	squamule width	USNM125084	2639
Prototaxites honeggeri	squamule width	USNM125084	2560
Prototaxites honeggeri	skeletal hypha width	UOF123868	15
Prototaxites honeggeri	skeletal hypha width	UOF123868	15
Prototaxites honeggeri	skeletal hypha width	UOF123868	10
Prototaxites honeggeri	skeletal hypha width	UOF123868	16
Prototaxites honeggeri	skeletal hypha width	UOF123868	15
Prototaxites honeggeri	skeletal hypha width	UOF123868	9

Prototaxites honeggeri	skeletal hypha width	OUF123854	8
Prototaxites honeggeri	skeletal hypha width	OUF123854	8
Prototaxites honeggeri	skeletal hypha width	OUF123854	8
Prototaxites honeggeri	skeletal hypha width	OUF123854	12
Prototaxites honeggeri	skeletal hypha width	OUF123854	9
Prototaxites honeggeri	skeletal hypha width	OUF123854	9
Prototaxites honeggeri	skeletal hypha width	OUF123854	10
Prototaxites honeggeri	skeletal hypha width	OUF123854	10
Prototaxites honeggeri	skeletal hypha width	OUF123854	10
Prototaxites honeggeri	skeletal hypha width	OUF123854	8
Prototaxites honeggeri	skeletal hypha width	OUF123854	9
Prototaxites honeggeri	skeletal hypha width	OUF123854	8
Prototaxites honeggeri	skeletal hypha width	OUF123854	7
Prototaxites honeggeri	skeletal hypha width	OUF123854	9
Prototaxites honeggeri	skeletal hypha width	OUF123854	10
Prototaxites honeggeri	skeletal hypha width	OUF123854	11
Prototaxites honeggeri	skeletal hypha width	OUF123854	11
Prototaxites honeggeri	skeletal hypha width	OUF123854	9
Prototaxites honeggeri	skeletal hypha width	OUF123854	9
Prototaxites honeggeri	skeletal hypha width	OUF123854	10
Prototaxites honeggeri	skeletal hypha width	OUF123854	12
Prototaxites honeggeri	skeletal hypha width	OUF123854	8
Prototaxites honeggeri	generative hypha width	OUF123854	2
Prototaxites honeggeri	generative hypha width	UOF123868	4
Prototaxites honeggeri	generative hypha width	UOF123868	5
Prototaxites honeggeri	generative hypha width	UOF123868	4
Prototaxites honeggeri	generative hypha width	UOF123868	4
Prototaxites honeggeri	generative hypha width	UOF123868	5
Prototaxites honeggeri	generative hypha width	UOF123868	5
Prototaxites honeggeri	generative hypha width	UOF123868	4
Prototaxites honeggeri	generative hypha width	UOF123868	3
Prototaxites honeggeri	generative hypha width	UOF123868	4
Prototaxites honeggeri	generative hypha width	OUF123854	3
Prototaxites honeggeri	generative hypha width	OUF123854	5
Prototaxites honeggeri	generative hypha width	OUF123854	4
Prototaxites honeggeri	generative hypha width	OUF123854	3
Prototaxites honeggeri	generative hypha width	OUF123854	4
Prototaxites honeggeri	generative hypha width	OUF123854	3
Prototaxites honeggeri	generative hypha width	OUF123854	3
Prototaxites honeggeri	generative hypha width	OUF123854	6
Prototaxites honeggeri	generative hypha width	OUF123854	4
Prototaxites honeggeri	generative hypha width	OUF123854	5
Prototaxites honeggeri	generative hypha width	OUF123854	6
Prototaxites honeggeri	generative hypha width	OUF123854	5
Prototaxites honeggeri	generative hypha width	OUF123854	3
Prototaxites honeggeri	generative hypha width	OUF123854	6
Prototaxites honeggeri	generative hypha width	OUF123854	5
Prototaxites honeggeri	generative hypha width	OUF123854	4
Prototaxites honeggeri	generative hypha width	OUF123854	4
Prototaxites honeggeri	generative hypha width	OUF123854	4
Prototaxites honeggeri	generative hypha width	OUF123854	3
Prototaxites honeggeri	generative hypha width	OUF123854	5
Prototaxites honeggeri	generative hypha width	OUF123854	3
Prototaxites honeggeri	generative hypha width	OUF123854	3
Prototaxites honeggeri	generative hypha width	OUF123854	4
Prototaxites honeggeri	generative hypha width	OUF123854	3
Prototaxites honeggeri	generative hypha width	OUF123854	3
Prototaxites honeggeri	generative hypha width	OUF123854	4
Prototaxites honeggeri	generative hypha width	OUF123854	4
Prototaxites honeggeri	generative hypha width	OUF123854	4
Prototaxites honeggeri	generative hypha width	OUF123854	3
Prototaxites honeggeri	photobiont diameter	UOF123868	9
Prototaxites honeggeri	photobiont diameter	UOF123868	9
Prototaxites honeggeri	photobiont diameter	UOF123868	8
Prototaxites honeggeri	photobiont diameter	UOF123868	8
Prototaxites honeggeri	photobiont diameter	UOF123868	7

in thalloid plants. Early land plants are all small and include minute balloonworts (*Janegraya*) and moss–like plants (*Dollyphyton, Edwardsiphyton*). The most distinctive plants are the hornwort *Casterlorum*, whose tall sporangia curled tightly when dehisced.

CONCLUSIONS

The Douglas Dam Lagerstätte at last allows visualization of Middle Ordovician (460 Ma) terrestrial vegetation. These fossil plants of a dolomitic paleokarst landscape are unlikely to have been representative of Ordovician vegetation in general, because other kinds of fossil plants are found in red beds of well drained aridland paleosols (Retallack, 2009), and in drab siltstones of fluvial and coastal wetlands (Retallack, 2015a). This paleokarst flora of Douglas Dam was dominated by *Casterlorum crispum* (hornwort), whereas well drained Ordovician soils were dominated by *Farghera robusta* (foliose lichens: Retallack, 2009), and waterlogged soils by *Prototaxites honeggeri* (nematophytes: Retallack, 2015a).

This evaluation of the Douglas Dam flora reveals that hornworts, liverworts, and mosses may have been distinct by 460 Ma, but recalibration of molecular clocks for early land plants (Morris *et al*., 2018) will be difficult due to lack of needed characters in these preserved fossils. The presence of hornworts, liverworts and mosses by 460 Ma does not resolve the many phylogenetic hypotheses concerning their relationships (Puttick *et al*., 2018). Provisional family assignments given here are well nested within more detailed bryophyte trees (Forrest *et al*., 2006; Wickett *et al*., 2014), thus raising addition problems with molecular clocks for the adaptive radiation of bryophytes.

A deeper understanding of Ordovician vegetation has ramifications for further understanding of Earth system science. Pot experiments with mosses (Porada *et al*., 2016) have demonstrated acceleration of chemical weathering that may have fuelled the Great Ordovician Biodiversification Event (GOBE: Harper *et al*., 2015), and ushered in the Hirnantian Ice Age (LeHeron & Craig, 2008; Lenton *et al*., 2012, Retallack, 2015a). This study lends support to the idea

that the Cambrian Explosion extended beyond the evolution of marine biota to also include land plants (Morris *et al*., 2018). Evolutionary advances of life and chemical weathering on land may have provisioned Cambrian and Ordovician marine evolution (Retallack, 2009, 2015a).

Acknowledgements—*Valuable assistance with collections was rendered by C. Brett and T. Paton at the University Cincinnati, by B. Hunda and G. Storrs at the Cincinnati Museum Center, and by K. Hollis and D. Levin and the U. S. Natural History Museum of the Smithsonian Institution. Light photomicrographs were obtained in the Center for Advanced Characterization of Oregon (CAMCOR), with assistance of J. Donovan, in the laboratory of D. Libuda, with assistance of N. Kurhanewicz–Codd, and of D. Gavin with assistance of C. Saban, all at the University of Oregon.*

REFERENCES

Ahmadjian V 1967. A guide to the algae occurring as lichen symbionts: isolation, culture, cultural physiology and identification. Phycologia 6: 127–160.

Anderson HM 1976. A review of the Bryophyta from the Upper Triassic Molteno Formation, Karoo Basin, South Africa. Palaeontologia Africana 19: 21–30.

Andrews HN 1960. Notes on Belgian specimens of *Sporogonites*. Palaeobotanist 7: 85–89.

Arbey F & Koeniguer J–C 1979. Les némathophyes et les algueraies de l'Ordovicien et du Dévonien Saharien. Bulletin Centre Recherche Exploracrion Produccion Elf Aquitaine 3: 409–418.

Argast S 1992. Enigmatic tubes in Ordovician limestones of the Mohawk Valley, New York. Palaios 7: 532–539.

Arnold CA 1952. A specimen of *Prototaxites* from Kettle Point black shale, Ontario. Palaeontographica B93: 45–56.

Banks HP 1975. Early vascular land plants: proof and conjecture. BioScience 25: 730–737.

Bonfante P & Selosse MA 2010. A glimpse into the past of land plants and of their mycorrhizal affairs: from fossils to evo-devo. New Phytologist 186: 267–270.

Boyce CK, Hotton CL, Fogel ML, Cody GD, Hazen RM, Knoll AH & Hueber FM 2007. Devonian landscape heterogeneity recorded by a giant fungus. Geology 25: 399–402.

Bradshaw MA 1981. Paleoenvironmental interpretations and systematics of Devonian trace fossils from the Taylor Group (lower Beacon Supergroup), Antarctica. New Zealand Journal of Geology and Geophysics 24: 615–652.

Braun A 1864. Nebst einer übersicht naturlichen Pflanzen systems. *In*: Ascherson PFA (Editor), Flora der Provinz Brandenberg, der Altmark und des Herzogthums Magdeburg. Birschwalb, Berlin: 22–101.

Bridge J 1955. Disconformity between Lower and Middle Ordovician Series at Douglas Lake, Tennessee. Geological Society of America Bulletin 66: 725–730.

Brown JT & Robinson CR 1976. Observations on the structure of *Marchantiolites blairmorensis* (Berry) n. comb. from the Lower Cretaceous of Montana, U. S. A. Journal of Paleontology 50: 309–311.

Brown RC, Lemmon BE & Carothers ZB 1982. Spore wall ultrastructure of *Sphagnum lescurii* Sull. Review of Palaeobotany and Palynology 38: 99–107.

Brubaker LB, Anderson PM, Murray BM & Koo D 1998. A palynological investigation of true–moss (Bryidae) spores: morphology and occurrence in modern and late Quaternary lake sediments of Alaska. Canadian Journal of Botany 76: 2145–2157.

Carafa A, Duckett JG & Ligrone R 2003. Subterranean gametophytic axes in the primitive liverwort *Haplomitrium* harbour a unique type of endophytic association with aseptate fungi. New Phytology 160: 185–197.

Cardona–Correa C, Piotrowski MJ, Knack JJ, Kodner RE, Geary DH & Graham LE 2016. Peat moss–like vegetative remains from Ordovician carbonates. International Journal of Plant Science 177: 523−538.

Caster KE & Brooks HK 1956. New fossils from the Canadian–Chazyan (Ordovician) hiatus in Tennessee. Bulletin of American Paleontology 36: 157–199.

Cavers F 1910. The inter–relationships of the Bryophyta. New Phytology 9: 269–304.

Conway Morris SC & Collins DH 1996. Middle Cambrian ctenophores from the Stephen Formation, British Columbia, Canada. Royal Society of London Philosophical Transacations B351: 279–308.

Crandall–Stotler B & Stotler RE 2000. Morphology and classification of the Marchantiophyta. *In*: Shaw AJ & Goffinet B (Editors), Bryophyte biology. Cambridge University Press, Cambridge: 21–49.

Crandall–Stotler B, Stotler RE & Long DG 2009. Morphology and classification of the Marchantiophyta. *In*: Goffinet B & Shaw AJ (Editors)—Bryophyte Biology. Cambridge University Press, Cambridge: 1–54.

Cridland AA & Williams JL 1966. Plastic and epoxy transfers of fossil plant compressions. Torrey Botanical Club Bulletin 93: 311–322.

Cronquist A, Takhtajan A & Zimmermann W 1966. On the higher taxa of Embryophyta. Taxon 15: 129–134.

Cross AT, Gillespie WH & Taggart RE 1996. The fossil plants of Ohio: overview and non–vascular plants. *In*: Feldman RM & Hackathorn M (Editors)—Fossils of Ohio. Ohio Division of Geological Survey Bulletin 26: 370–395

Davies NS, Gibling MR & Rygel MC 2011. Alluvial facies evolution during the Palaeozoic greening of the continents: case studies, conceptual models and modern analogues. Sedimentology 58: 220–258.

Dawson JW 1859. On the fossil plants from the Devonian rocks of Canada. Royal Society of London Quarterly Journal 15: 477–488.

Desirò A, Duckett JG, Pressel S, Villarreal JC & Bidartondo MI 2013. Fungal symbioses in hornworts: a chequered history. Royal Society of London Proceedings B280: e20130207.

Drinnan AN & Chambers TC 1986. Flora of the Lower Cretaceous Koonwarra Fossil Bed (Korumburra Group), South Gippsland, Victoria. Association of Australasian Palaeontologists, Memoir 3: 1–77.

Duff RJ, Villarreal JC, Cargill DC & Renzaglia KS 2007. Progress and challenges in hornwort phylogenetic reconstruction. Bryologist 110: 214–243.

Dunlop JA, Anderson LI & Braddy SJ 2003. A redescription of *Chasmataspis laurencii* Caster and Brooks, 1956 (Chelicerata: Chasmataspidida) from the Middle Ordovician of Tennessee, USA, with remarks on chasmataspid phylogeny. Royal Society of Edinburgh Transactions Earth Sciences 94: 207–225.

Edwards D & Axe L 2012. Evidence for a fungal affinity for *Nematasketum*, a close ally of *Prototaxites*. Botanical Journal of the Linnean Society 168: 1–18.

Edwards D, Fanning U & Richardson JB 1994. Lower Devonian coalified sporangia from Shropshire: *Salopella* Edwards & Richardson and *Tortilicaulis* Edwards. Botanical Journal of the Linnean Society 116: 89–110.

Edwards D, Morris JL, Richardson JB & Kenrick P 2014. Cryptospores and cryptophytes reveal hidden diversity in early land floras. New Phytologist 202: 50–78.

Epstein AG, Epstein JB & Harris LD 1977. Conodont color alteration: an index to organic metamorphism. U.S. Geological Survey Professional Paper 995: 1–27.

Fleischer M 1920. Natürliches System der Laubmoose. Hedwigia 61: 390–400.

Flowers S 1973. Mosses of Utah and the west. Brigham Young University Press, Provo: 567 pp.

Forrest LL, Davis EC, Long DG, Crandall–Stotler BJ, Clark A & Hollingsworth ML 2006. Unraveling the evolutionary history of the

liverworts (Marchantiophyta): multiple taxa, genomes and analyses. The Bryologist 109: . 303–335.
Fox PP & Grant LF 1944. Ordovician bentonites in Tennessee and adjacent states. Journal of Geology 52: 319–332.
Fritsch A 1908. Problematica Silurica. Raimund Gerhard, Leipzig: 28 pp.
Gray J 1985. The microfossil record of early land plants: advances in understanding of early terrestrialization, 1970–1984. Royal Society of London Philosophical Transacations B309: 167–195.
Gray J 1988. Evolution of the freshwater ecosystem: the fossil record. Palaeogeography, Palaeoclimatology, Palaeoecology 62: 1–214.
Gray J & Boucot AJ 1972. Palynological evidence bearing on the Ordovician–Silurian paraconformity in Ohio. Geological Society of America Bulletin 83: 1299–1314.
Gray J & Boucot AJ 1977. Early vascular land plants: proof and conjecture. Lethaia 10: 145–174.
Gray J, Massa D & Boucot AJ 1982. Caradocian land plant microfossils from Libya. Geology 10: 197–201.
Greguss P 1962. Some new data on the Ordovician land plants from Poland. Acta Biologica Universitas Szeged 8: 45–58.
Guerrak S 1988. Paleozoic marine sedimentation and associated oolitic iron–rich deposits, Tassili n'Ajjer and Illizi Basin, Saharan Platform, Algeria. Eclogiiae Geologica Helvetica 81: 457–485.
Guo CQ, Edwards D, Wu PC, Duckett JG, Hueber FM & Li CS 2012. *Riccardiothallus devonicus* gen. *et* sp. nov. , the earliest simple thalloid liverwort from the Lower Devonian of Yunnan, China. Review of Palaeobotany and Palynology 176: 35–40.
Harper DA, Zhang RB & Jin J 2015. The Great Ordovician Biodiversification Event: reviewing two decades of research on diversity's big bang illustrated by mainly brachiopod data. Palaeoworld 24: 75–85.
Hässel de Menendez GG 1986. *Leiosporoceras* Hässel n. gen. and Leosporocerotaceae Hässel n. fam. of Anthocerotopsida. Journal of Bryology 14: 255–259.
Hässel de Menendez GG 1988. Proposal for a new classification of genera within Anthocerotophyta. Journal of the Hattori Botanical Laboratory 64: 71–86.
Hawksworth DL 1988. The variety of fungal–algal symbioses, their evolutionary significance and the nature of lichens. Botanical Journal of the Linnaean Society London 96: 3–20.
Haynes CC 1910. *Sphaerocarpos hians* sp. nov., with a revision of the genus and illustrations of the species. Torrey Botancal Club Bulletin 37: 215–230.
Heeg M 1891. Niederösterreiche Lebermoose. Verhandlungen Zoologisch–Botancish Gesellschaft Wien 41: 567–573.
Hemsley AR 1989. The ultrastructure of the spore wall of the Triassic bryophyte *Naiadita lanceolata*. Review of Palaeobotany and Palynology 61: 89–99.
Henley WJ, Hironaka JL, Guillou L, Buchheim MA, Buchheim JA, Fawley MW & Fawley KP 2004. Phylogenetic analysis of the '*Nannochloris*–like' algae and diagnoses of *Picochloris oklahomensis* gen. et sp. nov. (Trebouxiophyceae, Chlorophyta). Phycologia 43: 641–652.
Hernick LV, Landing E & Bartowski KE 2008. Earth's oldest liverworts–*Metzgeriothallus sharonae* sp. nov. from the Middle Devonian (Givetian) of eastern New York, USA. Review of Palaeobotany and Palynology 148: 154–162.
Herrmann A & Haynes JT 2015. Ordovician of the Southern Appalachians, USA. Pre–Symposium Field Trip Stratigraphy 12: 203–251.
Hibbett DS, Binder M, Bischoff JF, Blackwell M, Cannon PF, Eriksson OE, Huhndorf S, James T, Kirk PM, Lücking R & Lumbsch HT 2007. A higher–level phylogenetic classification of the Fungi. Mycological Research 111: 509–547.
Høeg OA 1942. The Downtonian and Devonian flora of Spitsbergen. Norges Svalbard Ishavs og Undersøkelser Skrifter 83: 1–228.
Hoffman GL & Stockey RA 1997. Morphology and paleoecology of *Ricciopsis speirsae* sp. nov. (Ricciaceae), a fossil liverwort from the Paleocene Joffre Bridge locality, Alberta, Canada. Canadian Journal of Botany 75: 1375–1381.
Honegger R, Edwards D, Axe L & Strullu–Derrien C 2018. Fertile *Prototaxites taiti*: a basal ascomycete with inoperculate, polysporous asci lacking croziers. Royal Society Philosophical Transactions B373: e20170146.
Hou XG, Aldridge R, Bergstrom J, Siveter DJ, Siveter D & Feng XH 2017. The Cambrian fossils of Chengjiang, China: the flowering of early animal life. Wiley, Chichester: 316 pp.
Hueber FM 1961. *Hepaticites devonicus* a new fossil liverwort from the Devonian of New York. Missouri Botanical Garden Annals 48: 125–131.
Hueber FM 2001. Rotted wood–alga–fungus: the history and life of *Prototaxites* Dawson 1859. Review of Palaeobotany and Palynology 116: 123–158.
Huff WD 1983. Correlation of Middle Ordovician K–bentonites based on chemical fingerprinting Journal of Geology 91: 657–669.
Huff WD 2008. Ordovician K–bentonites: Issues in interpreting and correlating ancient tephras. Quaternary International 178: 276–287.
Huff WD & Turkmenoglu AG 1981. Chemical characteristics and origin of Ordovician K–bentonites along the Cincinnati Arch. Clays and Clay Minerals 29: 113.
Huff WD, Bergström SM & Kolata DR 1992. Gigantic Ordovician volcanic ash fall in North America and Europe: Biological, tectonomagmatic, and event–stratigraphic significance. Geology 20: 875–878.
Huff WD, Davis D, Bergstrom SM, Krekeler MPS, Kolata DR & Cingolani C 1997. A biostratigraphically well–constrained K–bentonite U–Pb zircon age of the lowermost Darriwilian Stage (Middle Ordovician) from the Argentine Precordillera. Episodes 20: 29–33.
Huff WD, Bergström SM & Kolata DR 2010. Ordovician explosive volcanism. *In*: Finney SC & Berry WBN (Editors)—The Ordovician Earth System. Geological Society of America Special Paper 466: . 13–28.
Janczkewski E 1872. Vergleichende Untersuchungen über die Entwicklungsgeschichte des Archegonium. Botanische Zeitschriift 30: 377–443.
Kenrick P, Wellman CH, Schneider H & Edgecombe G 2012. A timeline for terrestrialization: consequences for the carbon cycle in the Palaeozoic. Royal Society of London Philosophical Transactions 367: 519–536.
Kozlowski R & Greguss P 1959. Discovery of Ordovician land plants. Acta Palaeontologica Polonica 4: 1–9.
Krassilov V 1981. *Orestovia* and the origin of vascular plants. Lethaia 14: 235–250.
Krings ML, Taylor TN & Harper C 2017. Early fungi: evidence from the fossil record. *In*: Dighton J & White JF (Editors)—The fungal community: its organization and role in the ecosystem. CRC Press, Boca Raton: 37–52
Kříž J & Pojeta J 1974. Barrande's colonies concept and a comparison of his stratigraphy with the modern stratigraphy of the middle Bohemian Lower Palaeozoic rocks (Barrandian) of Czechoslovakia. Journal of Paleontology 48: 489–494.
Lang WH 1937. On the plant remains from the Downtonian of England and Wales. Royal Society of London Philosophical Transacations B227: 245–329.
Laurence RA 1944. An early Ordovician sinkhole deposit of volcanic ash and fossiliferous sediments in east Tennessee. Journal of Geology 52: 235–249.
Le Hérissé A, Vecoli M, Guidat C, Not F, Breuer P, Wellman C & Steemans P 2017. Middle Ordovician acritarchs and problematic organic–walled microfossils from the Saq–Hanadir transitional beds in the QSIM–801 well, Saudi Arabia. Revue Micropaléontologique 60: 289–318.
Le Heron DP & Craig J 2008. First–order reconstruction of a Late Ordovician Saharan ice sheet. Geological Society of London Journal 165: 19−29.
Lenton TM, Crouch M, Johnson M, Pires N & Dolan L 2012. First plants cooled the Ordovician. Nature Geoscience 5: 86–90.
Lesquereux L 1874. On remains of land plants in the Lower Silurian. American Journal of Science and Arts 7: 3.
Lesquereux L 1877. Land plants, recently discovered in the Silurian rocks of the United States. American Philosophical Society Proceedings 17: 163–173.
Li R, Sun B, Wang H, He Y, Yang G, Yan D & Lin Z 2014. *Marchantites huolinhensis* sp. nov. (Marchantiales)–A new fossil liverwort with gemma cups from the Lower Cretaceous of Inner Mongolia, China. Cretaceous

Research 50: 16–26.
Li RY, Wang XL, Chen JW, Deng SH, Wang ZX, Dong JL & Sun BN 2016. A new thalloid liverwort: *Pallaviciniites sandaolingensis* sp. nov. from the Middle Jurassic of Turpan–Hami Basin, NW China. PalZ 90: 389–397.
Libertin M, Kvaček J, Bek J, Žárský V & Štorch P 2018. Sporophytes of polysporangiate land plants from the early Silurian may have been photosynthetically autonomous. Nature Plants 4: 269–271.
Ligrone R, Carafa A, Lumini E, Bianciotto V, Bonfante P & Duckett JG 2007. Glomeromycotean associations in liverworts: a molecular, cellular, and taxonomic analysis. American Journal of Botany 94: 1756–1777.
Limpricht G 1876. Laub–und Lebermoose. *In*: Cohn F (Editor)—Kryptogamen–Flora von Schlesien. Kern, Breslau, Volume 1: 225–352.
Lindley J 1836. A Natural System of Botany. Longman, London: 526 pp.
Linnaeus C von 1753. Species plantarum. Laurentii Salvii, Holmiae: 1568 pp.
McMahon WJ & Davies NS 2018. Evolution of alluvial mudrock forced by early land plants. Science 359: 1022–1024.
McQueen CB 1985. Morphology of four species of *Sphagnum* in Section *Acutifolia*. The Bryologist 88: 1–4.
Min K, Renne PR & Huff WD 2001. $^{40}Ar/^{39}Ar$ dating of Ordovician K–bentonites in Laurentia and Baltoscandia. Earth and Planetary Science Letters 185: 121–134.
Moore RT 1980. Taxonomic proposals for the classification of marine yeasts and other yeast–like fungi including the smuts. Botanica Marina 23: 361–373.
Morris JL, Puttick MN, Clark JW, Edwards D, Kenrick P, Pressel S, Wellman CH, Yang Z, Schneider H & Donoghue PC 2018. The timescale of early land plant evolution. U.S. National Academy of Sciences Proceedings 115: e2274–2283.
Morton JB & Benny GL 1990. Revised classification of arbuscular mycorrhizal fungi (Zygomycetes): a new order, Glomales, two new suborders, Glomineae and Gigasporineae, and two families, Acaulosporaceae and Gigasporaceae, with emendation of Glomaceae. Mycotaxon 37: 471–491.
Němejc F & Pacltova B 1974. Hepaticae in the Senonian of South Bohemia. Palaeobotanist 21: 23–26.
Neuburg MF 1960. Mosses feuillées des couches Permiennes de l'Angaride. Travail Institut Géologique Academie Sciences U. R. S. S. 19: 1–104.
Neuman RB 1955. Middle Ordovician rocks of the Tellico–Sevier Belt, eastern Tennessee. U.S. Geologial Survey Professional Paper 274F: 141–178.
Newsham KK 2010. The biology and ecology of the liverwort *Cephaloziella varians* in Antarctica. Antarctic Science 22: 131–143.
Nøhr–Hansen H & Koppelhus EB 1988. Ordovician spores with trilete rays from Washington Land, North Greenland. Review of Palaeobotany and Palynology 56: 305–311.
Novikoff A & Barabasz–Krasny B 2015. Modern plant systematics: General issues. Liga–Press, Lviv: 685 pp.
Oostendorp C 1987. The bryophytes of the Palaeozoic and Mesozoic. Bryophyta Bibliotheca 34: 1–112.
Pant DD & Bhowmik N 1998. Fossil bryophytes–with special reference to Gondwanaland forms. *In*: Chopra RN (Editor)—Topics in bryology. Allied Publishers, New Delhi: 1–52.
Pax F 1900. Prantl's Lehrbuch der Botanik. Ed. 11. Wilhelm Engelmann, Leipzig: 478 pp.
Perry E, Paytan A, Pedersen B & Velazquez–Oliman G 2009. Groundwater geochemistry of the Yucatan Peninsula, Mexico: constraints on stratigraphy and hydrogeology. Journal of Hydrology 367: 27–40.
Porada P, Lenton TM, Pohl A, Weber B, Mander L, Donnadieu Y, Beer C, Pöschl U & Kleidon A 2016. High potential for weathering and climate effects of non–vascular vegetation in the Late Ordovician. Nature Communications 7: e12113.
Puttick MN, Morris JL, Williams TA, Cox CJ, Edwards D, Kenrick P, Pressel S, Wellman CH, Schneider H, Pisani D & Donoghue PC 2018. The interrelationships of land plants and the nature of the ancestral embryophyte. Current Biology 28: 1–13.
Redecker D, Kodner R & Graham LE 2000. Glomalean fungi from the Ordovician. Science 289: 1920–1921.
Redecker D, Kodner R & Graham LE 2002. *Palaeoglomus grayi* from the Ordovician. Mycotaxon 84: 33–37.
Retallack GJ 2000. Ordovician life on land and early Paleozoic global change. *In*: Gastaldo RA & DiMichele WA (Editors)—Phanerozoic ecosystems. Paleontological Society Paper 6: 21−45.
Retallack GJ 2001a. Soils of the past. Blackwell, Oxford: 403 pp.
Retallack GJ 2001b. *Scoyenia* burrows from Ordovician paleosols of the Juniata Formation in Pennsylvania. Palaeontology 44: 209–235.
Retallack GJ 2008. Cambrian paleosols and landscapes of South Australia. Australian Journal of Earth Science 55: 1083–1106.
Retallack GJ 2009. Cambrian–Ordovician non–marine fossils from South Australia. Alcheringa 33: 355–391.
Retallack GJ 2015a. Late Ordovician glaciation initiated by early land plant evolution, and punctuated by greenhouse mass–extinctions. Journal of Geology 123: 509–538.
Retallack GJ 2015b. Acritarch evidence of a late Precambrian adaptive radiation of Fungi. Botanica Pacifica 4: 19–33.
Retallack GJ 2015c. Silurian vegetation stature and density inferred from fossil soils and plants in Pennsylvania, U.S.A. Geological Society of London Journal 172: 693–709.
Retallack GJ 2018. *Dickinsonia* steroids not unique to animals. Science 361: 1246, eletter to doi: 10. 1126/science. aat7228.
Retallack GJ & Landing E 2014. Affinities and architecture of Devonian trunks of *Prototaxites loganii*. Mycologia 106: 1143–1156.
Retallack GJ, Dunn KL & Saxby J 2013a. Problematic Mesoproterozoic fossil *Horodyskia* from Glacier National Park, Montana, USA. Precambrian Research 226: 125–142.
Retallack GJ, Krull ES, Thackray GD & Parkinson D 2013b. Problematic urn–shaped fossils from a Paleoproterozoic (2.2 Ga) paleosol in South Africa. Precambrian Research 235: 71–87.
Rickards RB 2000. The age of the earliest clubmosses: the Silurian *Baragwanathia* flora, Victoria, Australia. Geological Magazine 137: 207–209.
Rubinstein CV & Vaccari NE 2004. Cryptospore assemblages from the Ordovician/Silurian Boundary in the Puna Region, North-west Argentina. Palaeontology 47: 1037–1061.
Rubinstein CV, Gerrienne P, de la Puente G, Astini RA & Steemans P 2010. Early Middle Ordovician evidence for land plants in Argentina (eastern Gondwana). New Phytologist188: 365–369.
Salamon MA, Gerrienne P, Steemans P, Gorzelak P, Filipiak P, Le Hérissé A, Paris F, Cascales-Miñana B, Brachaniec T, Misz-Kennan M & Niedźwiedzki R 2018. Putative Late Ordovician land plants. New Phytologist 218: 1305–1309.
Schimper WP 1843. Bryologia europeae. Schweitzerbartsche, Stuttgart: 13 pp.
Schimper WP 1857. Mémoire pour servir à l'histoire naturelle des Sphaignes (*Sphagnum* L.). Imprimerie Impériale, Paris: 96 pp.
Schmid R 1976. Septal pores in *Prototaxites*, an enigmatic Devonian plant. Science 191: 287–288.
Schuster RM 1956. Notes on Nearctic Hepaticae X. A study of *Cephaloziella rhizantha*, *C. floridae* and *C. ludoviciana*. The Bryologist 59: 130–140.
Schweitzer H–J 1983. Die Unterdevonfloren des Rheinlandes Palaeontographica B189: 1–138.
Seilacher A 2007. Trace fossil analysis. Springer, Berlin: 226 pp.
Sell BK, Samson SD, Mitchell CE, McLaughlin PI, Koenig AE & Leslie SA 2015. Stratigraphic correlations using trace elements in apatite from Late Ordovician (Sandbian–Katian) K–bentonites of eastern North America. Geological Society of America Bulletin 127: 1259–1274.
Shaw AJ, Cox CJ, Buck WR, Devos N, Buchanan AM, Cave L, Seppelt R, Shaw B, Larraín J, Andrus R & Greilhuber J 2010. Newly resolved relationships in an early plant lineage: Bryophyta Class Sphagnopsida (peat mosses). American Journal of Botany 97: 1511–1531.
Snigirevskaya IS, Popov LE & Zdeska D 1992. New discovery of the oldest higher plant remains in the Middle Ordovician of Kazakhstan (Novie nakhodni ostatkov dreveiischikh veschikh rastenii I srednem ordovike juusnogo kazakhstana). Botanicheskiii Zhurnal 77: 1–10.
Steemans P & Wellman CH 2018. A key for the identification of cryptospores. Palynology DOI: 10. 1080/01916122. 2017. 1411844 (2018).

Steemans P, Le Hérissé A, Melvin J, Miller MA, Paris F, Verniers J & Wellman CH 2009. Origin and radiation of the earliest vascular land plants. Science 324: 353–353.

Steemans P, Wellman CH & Gerrienne P 2010. Palaeogeography and paleoclimatic considerations based on Ordovician to Lochkovian vegetation. *In*: Vecoli M, Clément G & Meyer–Berthaud B (Editors)—The terrestrialization process: modelling complex interactions in the biosphere–geosphere interface. Geological Society of London Special Publication 339: 49–58

Steinhauff DM & Walker KR 1995. Recognizing exposure, drowning, and 'missed beats': Platform–interior to platform margin sequence stratigraphy of Middle Ordovician limestones, East Tennessee. Journal of Sedimentary Research B65: 183–207.

Stotler R & Crandall–Stotler B 1977. A checklist of the liverworts and hornworts of North America. The Bryologist 80: 405–428.

Strother PK 1991. Classification schema for the cryptospores. Palynology 15: 219–236.

Strother PK 2016. Systematics and evolutionary significance of some new cryptospores from the Cambrian of eastern Tennessee, USA. Review of Palaeobotany and Palynology 227: 28–41.

Strullu-Derrien C, Kenrick P, Pressel S, Duckett JG, Rioult JP & Strullu DG 2014. Fungal associations in Horneophyton ligneri from the Rhynie Chert (c. 407 million year old) closely resemble those in extant lower land plants: novel insights into ancestral plant–fungus symbioses. New Phytologist 203: 964–979.

Taylor J, Hollingsworth PJ & Bigelow WC 1974. Scanning electron microscopy of liverwort spores and elaters. The Bryologist 77: 281−327.

Taylor TN, Taylor EL & Krings M 2009. Paleobotany: the biology and evolution of fossil plants. Elsevier, Amsterdam: 1224 pp.

Taylor WA 1996. Ultrastructure of lower Paleozoic dyads from southern Ohio. Review of Palaeobotany and Palynology 92: 269–279.

Taylor WA 1997. Ultrastructure of lower Paleozoic dyads from southern Ohio II: Dyadospora murusattenuata, functional and evolutionary considerations. Review of Palaeobotany and Palynology 97: 1–8.

Taylor WA & Strother PK 2008. Ultrastructure of some Cambrian palynomorphs from the Bright Angel Shale, Arizona, USA. Review of Palaeobotany and Palynology 151: 41–50.

Taylor WA & Strother PK 2009. Ultrastructure, morphology, and topology of Cambrian palynomorphs from the Lone Rock Formation, Wisconsin, USA. Review of Palaeobotany and Palynology 153: 296–309.

Terasmae J 1955. On the spore morphology of some *Sphagnum* species. The Bryologist 58: 306–311.

Thomas WA & Astini RA 2003. Ordovician accretion of the Argentine Precordillera terrane to Gondwana: a review. Journal of South American Earth Science 16: 67–79.

Thompson CK, Kah LC, Astini R, Bowring SA & Buchwaldt R 2012. Bentonite geochronology, marine geochemistry, and the Great Ordovician Biodiversification Event (GOBE). Palaeogeography Palaeoclimatology Palaeoecology 321: 88–101.

Tomescu AMF & Rothwell GW 2006. Wetlands before tracheophytes; thalloid terrestrial communities of the Early Silurian Passage Creek biota (Virginia). *In*: Greb SF & DiMichele WA (Editors)—Wetlands through time. Geological Society of America Special Paper 399: 41–56.

Tomescu AMF, Pratt LM, Rothwell GW, Strother PK & Nadon GC 2009. Carbon isotopes support the presence of extensive land floras pre–dating the origin of vascular plants. Palaeogeography Palaeoclimatology Palaeoecology 283: 46–59.

Turland NJ, Wiersema JH, Barrie FR, Greuter W, Hawksworth DL, Herendeen PS, Knapp S, Kusber WH, Li DZ, Marhold K & May TW 2017. International Code of Nomenclature for algae, fungi, and plants (Shenzhen Code) adopted by the Nineteenth International Botanical Congress Shenzhen, China, July 2017. Regnum Vegetabile 159: 1–254.

Tyagi VVS 1975. The heterocysts of blue-green algae (Myxophyceae). Biological Reviews 50: 247–284.

Vavrdová M 1984. Some plant microfossils of possible terrestrial origin from the Ordovician of Central Bohemia. Vestnik Ustredniho Ustavu Geologickeho 59: 65–170.

Vecoli M, Delabroye A, Spina A & Hints O 2011. Cryptospore assemblages from Upper Ordovician (Katian–Hirnantian) strata of Anticosti Island, Québec, Canada, and Estonia: Palaeophytogeographic and palaeoclimatic implications. Review of Palaeobotany and Palynology 166: 76–93.

Vecoli M, Wellman CH, Gerrienne P, Le Hérissé A & Steemans P 2017. Middle Ordovician cryptospores from the Saq–Hanadir transitional beds in the QSIM–801 well, Saudi Arabia. Revue Micropaléontologique 60: 319–331.

Villarreal JC & Renzaglia KS 2006. Structure and development of *Nostoc* strands in *Leiosporoceros dussii* (Anthocerotophyta): a novel symbiosis in land plants. Amercan Journal of Botany 93: 693–705.

Walker C & Schüßler A 2004. Nomenclatural clarifications and new taxa in the Glomeromycota. Mycological Research 108: 981–982.

Walker KR, Steinhauff DM & Roberson KE 1992. Uppermost Knox Group, the Knox unconformity, the Middle Ordovician transition from shallow shelf to deeper basin at Dandridge, Tennessee. *In*: Driese SG, Mora CI & Walker KR (Editors)—Paleosols, Paleoweathering Surfaces, and Sequence Boundaries. University of Tennessee Department of Geology Studies in Geology 21: 13–18

Wang B, Yeun LH, Xue JY, Liu Y, Ané JM & Qiu YL 2010. Presence of three mycorrhizal genes in the common ancestor of land plants suggests a key role of mycorrhizas in the colonization of land by plants. New Phytologist 186: 514–525.

Wellman CH & Gray J 2000. The microfossil record of early land plants. Royal Society of London Philosophical Transactions B355: 717–732.

Wellman CH, Osterloff PL & Mohiuddin U 2003. Fragments of the earliest land plants. Nature 475: 282–285.

Wellman CH, Steemans P & Miller MA 2015. Spore assemblages from Upper Ordovician and lowermost Silurian sediments recovered from the Qusaiba–1 shallow corehole, Qasim region, central Saudi Arabia. Review of Palaeobotany and Palynology 212: 111–126.

Wickett NJ, Mirarab S, Nguyen N, Warnow T, Carpenter E, Matasci N, Ayyampalayam S, Barker MS, Burleigh JG, Gitzendanner MA & Ruhfel BR 2014. Phylotranscriptomic analysis of the origin and early diversification of land plants. U.S. National Academy of Sciences Proceedings 111: e4859–4868.

Zapomělová E, Hrouzek P, Řeháková K, Šabacká M, Stibal M, Caisová L, Komárková J & Lukešová A 2008. Morphological variability in selected heterocystous cyanobacterial strains as a response to varied temperature, light intensity and medium composition. Folia Microbiologica 53: 333–341.